Negative Skin Friction on Single Piles in Collapsible Soil

A Thesis

In

The Department of Building Civil Engineering and Environmental Engineering

Presented in Partial Fulfillment of the Requirements for the

Degree of Master of Applied Science at

Concordia University

Montreal, Quebec, CANADA

December 2009

Your file Votre référence
ISBN: 978-0-494-67251-8
Our file Notre référence
ISBN: 978-0-494-67251-8

ABSTRACT

Negative Skin Friction on Single Piles in Collapsible Soil

Ibrahim Mashhour

Collapsible soil is known as problematic soil, which possesses considerable strength when it is dry and loses its strength and experience excessive settlement when inundated. Geotechnical engineers face a great challenge when they build on/in collapsible soil. Inundation of collapsible soil may take place due to surface running water or raising the groundwater level. In case of surface water, the amount of settlement varies, depending on the extent of the wetting zone and the degree of saturation in the soil. The case of rising groundwater will produce full saturation in the ground and accordingly, the maximum settlement of the foundations.

In the literature, there is lack of sufficient and reliable methods for predicting drag force on piles embedded in collapsible soils. These difficulties stem from the fact modeling collapsible soil analytically is difficult at best, while collapsible soil is governed by the collapse potential of the soil and method of inundation.

In this thesis, the results of an experimental investigation on a single end-bearing pile embedded in collapsible soil will be presented. The objective of this experimental investigation was to measure the soil collapse and the associated settlement and accordingly the negative skin friction on the pile's shaft for a given soil and pile conditions due to soil inundation. Empirical formula is presented to estimate the negative skin friction on these piles for a given soil/pile condition.

ACKNOWLEDGEMENT

I dedicate this thesis to the soul of my Grandfather who passed away during the course of my study.

I would like to express my deep sincere gratitude and thanks to my supervisor Dr. Adel Hanna for his continuous support throughout my master program by all means, and I was so honored to work under his supervision.

I would like to thank my family for their patience, encouragement and support, and special thanks to my father who's love and unlimited support gave me the energy to complete this study.

I would like to Thank Dr. Taher Ayadat for his assistance. Last but not least I would like to thank my colleagues and the laboratory technicians in BCEE department, Concordia University, who have assisted me during my experimental investigation and special thanks to Sherif Soliman, Sarah Tahsin and Gustavo Guedez for their fruitful discussions during the experimental phase of this thesis.

TABLE OF CONTENTS

LIST OF FIGURES

LIST OF TABLES

CHAPTER 1

INTRODUCTION

1.1 Overview

The problem of negative skin friction (NSF) is the most common problem in the design of pile foundations in soft ground (Lee et al. 2001). In the literature, several reports can be found dealing with negative skin friction on pile foundations, the majority of them dealing with soft soils, while few address the case of collapsible soils, and accordingly, there is a high level of uncertainty for predicting negative skin force on these piles.

Negative skin friction mobilizes on piles when the surrounding soil's settlement is faster than the settlement of the pile, resulting in friction force acting downward on the pile shaft. Collapsible soil is known as unsaturated soil that experiences a significant reduction in volume upon wetting; therefore piles installed in collapsible soils are subjected to negative skin friction due to the excessive settlement accompanied during soil wetting.

The collapse behavior is governed by some parameters to include the collapse potential, the method of inundation and the thickness of the collapsible layer.

In this investigation, a prototype experimental model was built to measure negative skin friction forces acting on an end-bearing pile embedded in collapsible soil during inundation. The drag load on the pile shaft was measured as well as the governing parameters.

1.2. Thesis outline

A brief review of the literature on negative skin friction is presented in chapter two, followed by a description of the testing program and testing procedures in chapter three. The tests results and the analysis are presented in chapter four. Based on the results presented in this chapter, an analytical model was also presented in chapter four to predict the negative skin friction on these piles. Finally conclusions and recommendations are listed in chapter five.

CHAPTER 2

LITERATURE REVIEW

2.1. General

In this chapter the history of the negative skin friction on pile foundation is presented, with emphasis on piles installed in collapsible soils. It is essential that, before proceeding with this study, that collapsible soil is defined in this chapter briefly in terms of types, causes of collapse, collapse mechanism, and the parameters affecting collapse. Therefore there will be three main topics in this chapter as shown in the diagram below.

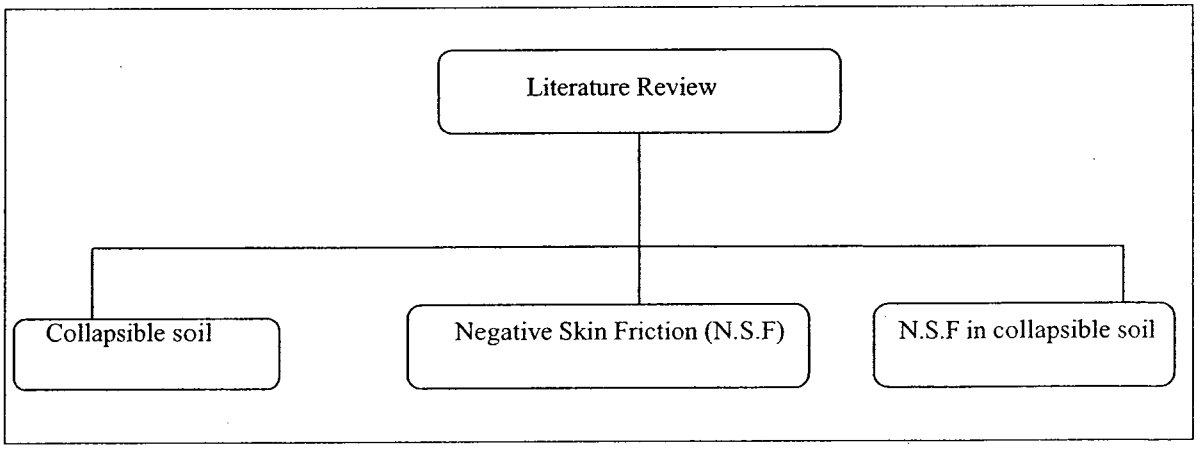

Fig.2.1. Literature review organization

2.2. Literature Review Pertinent to Collapsible Soils

Collapsible soil is a metastable material, traditionally defined as unsaturated soils that experiences a radical rearrangement of particles and significant reduction of volume upon wetting with or without additional loading (Bara 1976; Houston et al., 1988).

Collapsible soils are often located in arid regions, where soils are unsaturated. A wide range of soils fall into the category of collapsible soil, including naturally existing types of soils such as: Alluvial flood plains, mud flows, residual soils, colluvial deposits, fans, mud flows, aeolian or wind-blow deposits sands and silts (loess), volcanic tuffs, gypsum, dispersive clays, loose cemented sands , sodium rich montmorillonite clays (Clemence and Finbarr 1981), arid saline soils (sabkhas), and man-placed fills made of sands, ashes, random material such as construction debris, mine tailings, and coal ash fills.

There are many different causes of soil wetting and soil saturation, either as a result of urbanization or as a result of natural causes. Some of these causes of soil wetting can be controlled; however most of them cannot be controlled. Some of these possible sources of wetting are: groundwater level, rise, landscape irrigation, broken water pipelines or sewer lines, poor surface drainage, Intentional and unintentional groundwater recharge, damming due to cut/fill construction, and the moisture increase due to capillary rise.

Another classification of collapsible soils based their behavior under different loading conditions divides collapsible soils into two main types (Grigorian, 1997):

Type 1: On wetting undergo collapse under external loads (not self weight).

Type 2: Collapses under both self weight of overlying soils and external loads.

The collapse mechanism requires three main conditions as mentioned by (Barden et., al 1973):

A- An open potentially unstable partly saturated structure.

B- A sufficient applied or existing stress to develop metastable condition.

C- A strong soil bond that results from a cementing agent, soil suction or other bonding agent, stabilizing the contacts between granular particles, where these bonds weaken or break upon wetting with water leading to significant volume change "collapse".

Figure 2.2 presents the different types of inter-particle bonds for collapsible soils, the figure was presented by (Clemence and Finbarr, 1981) based on bond types suggested by (Barden et., al, 1973).

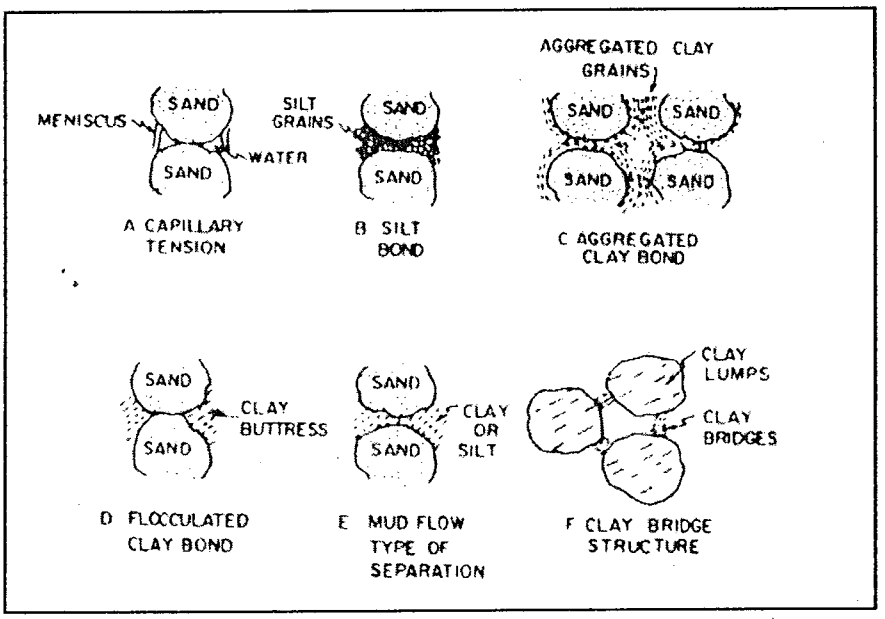

Fig.2.2. Typical collapsible soil structures (Clemence and Finbarr, 1981)

2.2.1. Parameters Affecting Collapse

There are numerous factors affecting the collapse potential of soils as (Houston and Houston, 1997) have listed, such as:

-Soil type (percentage of fines, soil fabric, mineral composition...etc)

-Compaction effort

-Initial water content

-Stress level at soaking (inundation pressure)

2.2.2. Collapsible Soil Identification

One of the simple procedures identifying the collapsible soil is through a factor known as the collapse potential C_P using the oedometer test was suggested by (Knight 1963), where the soil sample is being loaded at the natural moisture content on increments to a maximum load of 200 kPa at which the soil is being wetted and fully saturated with water, then left for 24 hours, the result of oedometer test for determining collapse potential can be expressed by the e-logp curve as shown in figure 2.3, and the collapse potential can be determined from the curve where it is equal to the deformation of soil due to the addition of water, divided by the initial height of the specimen, expressed in percent as presented in equation [2.1].

$$C_p = \frac{\Delta e_c}{1 + e_o} = \frac{\Delta H_c}{H_o} \ldots\ldots\ldots\ldots\ldots\ldots\ldots\ldots\ldots \quad [2.1]$$

Where Δe_c is the change in void ratio upon wetting, Δe_o is the natural void ratio, ΔH_c is the change in height upon wetting and H_o is the initial height of the specimen.

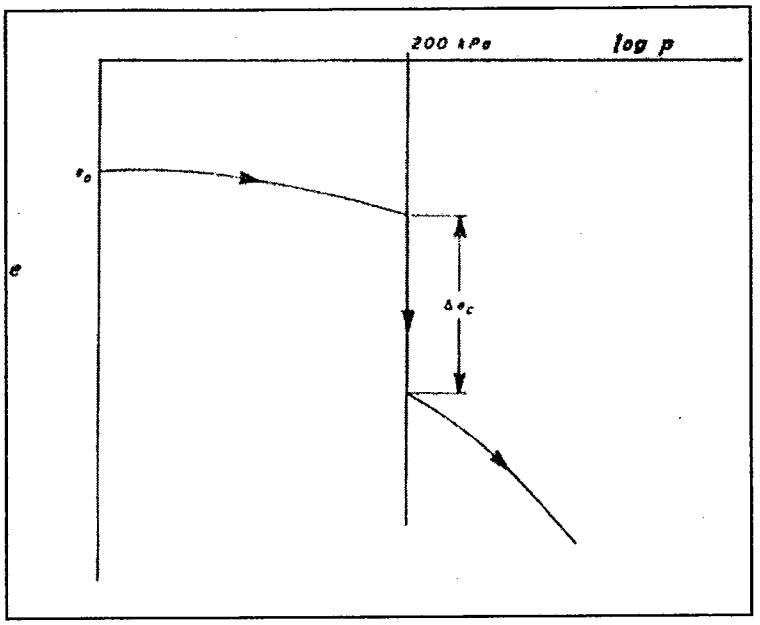

Fig.2.3. Typical collapse potential result (Clemence and Finbarr 1981)

A classification of collapsible soils according to severity of problem with respect to collapse potential is shown in the table 2.1, as introduced by (Jennings and Knight 1975). This classification made it easier to judge the severity of the problem based on the collapse potential determined from oedometer test.

Table 2.1.Relation of collapse potential to the severity of foundation problems (Jennings and Knight 1975)

C_p (%)	Severity of problem
0-1	No problem
1-5	Moderate trouble
5-10	Trouble
10-20	Severe trouble
>20	Very severe trouble

2.2.3. Mitigation Measures for Foundations on Collapsible Soils

The many different measures taken to avoid foundation failure have been studied by many researchers (Houston and Houston, 1997; Clemence and Finbarr, 1981; Beckwith, 1995; Evstatiev, 1995; Houston and Houston, 1989; Pengelly, et al., 1997; Rollins and Rogers, 1994; and Turnbull, 1968). These mitigation measures fall under the following categories:

- Removal and replacement of the collapsible soil layer
- Pile or pier foundations
- Avoidance of wetting
- Pre-wetting
- Controlled wetting
- Chemical stabilization or grouting
- Dynamic compaction
- Differential settlement resistant foundations

2.3. Literature Review Pertinent to Negative Skin Friction on Pile Foundations

2.3.1. General

Piles installed in deformable soils are susceptible to additional (indirect) load, and this occurs as a result of relative settlement between the pile and the surrounding soil and due to the friction between the two surfaces, where the soil settlement exceeds that of the pile. This additional (indirect) load known as "negative skin friction" or "drag load" can cause serious damages; as many cases have reported in history. Therefore the problem of negative skin friction has been a matter of interest to many researchers, and a very important aspect to be considered in pile design.

Lee et al.,(2001) stated that the problem of negative skin friction is considered to be the most common problem in the design of pile foundations in soft ground, and yet there is a lack of reliable satisfactory methods to compute such forces, as both empirical and elastic methods over estimate the NSF values. It was also reported by (Little and Ibrahim, 1993) that various researchers at the Wroth Memorial Symposium have predicted negative skin friction in a wide range of 98% to 515% of the measured value.

Since soil settlement is time dependent, especially in cohesive soils where consolidation takes place, therefore negative skin friction is time dependent as well, as numerous investigations including full-scale tests have shown (Johannessen and Bjerrum, 1965; Bjerrum et al., 1969; Fellenius and Broms, 1969; Endo et al., 1969; Bozozuk, 1972; Fellenius 1972; Walker et al. 1973).

It was also found that the magnitude of soil settlement has a great effect on negative skin friction; essentially, the larger the soil settlement, the greater the negative skin friction force (Poulos 1997; Lee et al., 2001).

Several elastic solutions have been suggested for predicting negative skin friction force (Poulos and Davis 1980; Chow et al. 1990; Lee 1993; Teh and Wong 1995), however Lee et al. (2002) have carried out a numerical analysis and marked the importance of soil slip at the pile-soil interface to be considered to provide an economic solution as the previous elastic solutions in general over predict the negative skin friction force acting on piles.

Various solutions were proposed in literature to reduce negative skin friction. Bjerrum et al., (1969) have suggested the cathodic protection (electro-osmosis) for steel piles, and compared the results to piles coated with bitumen. Coating piles with bitumen has shown to be more efficient and can be applied to almost all types of piles, unlike cathodic protection which can only be applied to steel piles. Many researchers have recommended the use of bitumen for pile coating as an effective solution for reducing negative skin friction (Bjerrum et al 1969; Fellenius 1972; Walker et al. 1973; Clemente 1981; Briaud 1997).

2.3.2. Literature Review Pertinent to Negative Skin Friction on Pile Foundations in Clays and Soft Soils

Terzaghi and Peck (1948) have introduced the equivalent footing concept for estimating pile group settlement, where it was assumed that the load the imposed by the building and carried by the piles, is entirely supported by a flexible raft located at the level of the lower third of the pile length, as shown in figure 2.4.

The study assumed that the drag load (negative skin friction) on pile shaft imposed by consolidating soil surrounding the pile, is acting on the entire length of the pile. Later on this assumption has shown to be rather conservative in case of floating piles, while it has been shown to be acceptable for end-bearing piles.

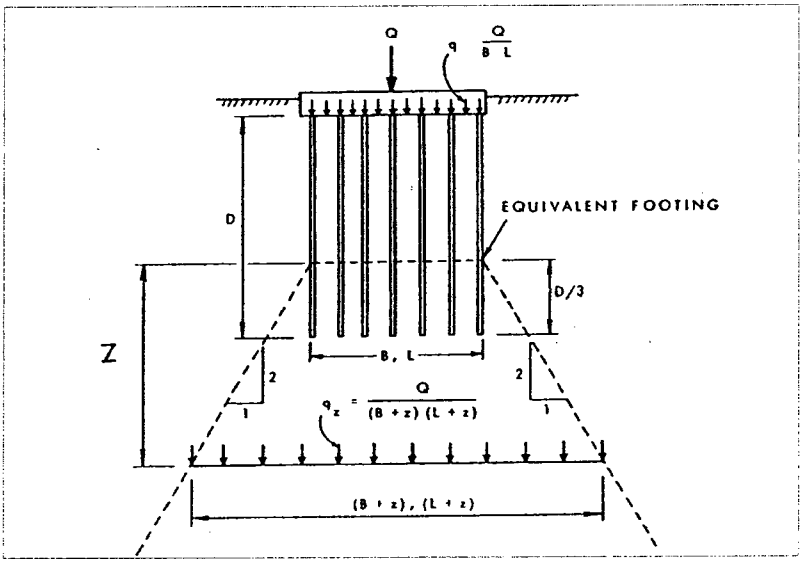

Fig. 2.4 Calculations of settlement for a pile group in homogenous clay soil using equivalent footing concept (Terzaghi and Peck, 1948)

Johannessen and Bjerrum (1965) have performed full scale tests on instrumented end-bearing steel piles subjected to negative skin friction caused by the consolidation of the surrounding soil. The excess pore water was measured and the effective stress was determined after full dissipation of excess pore water pressure. It was found that the negative skin friction is proportional to the effective earth pressure based on full-scale experiments on driven piles, and equation [2.2] was introduced, where τ_a is the negative skin friction force at any point along the pile length, σ'_v is the effective vertical stress, K is the coefficient of earth pressure and φ'_a is the effective angle of internal friction.

$$\tau_a = \sigma'_v K \tan \varphi'_a \quad \ldots\ldots\ldots\ldots\ldots\ldots\ldots\ldots\ldots \quad [2.2]$$

Later on the coefficient of negative skin friction β was introduced based on the effective stress concept introduced by Johannessen and Bjerrum (1965).

Fellenius (1972) has studied negative skin friction forces by obtaining full scale field measurements. The piles were installed in soft clay layers where a small regional settlement (consolidation settlement) in the clay layer had imposed the negative skin friction force on the piles. Axial loads and bending moments were measured through gauges installed in the piles as shown in figures 2.5 & 2.6. The distribution of axial forces along the pile shaft and the increase in load due to negative skin friction forces with depth were plotted as shown in figure 2.6 and 2.7. From the axial force measured and plotted, Fellenius was able to introduce a unit skin friction distribution along the pile length, where the upper layer is soft settling soil and the lower layer is non-settling soil as shown in figure 2.9.

Figure 2.8 assumes the negative skin friction force to be constant along the upper portion of the pile penetrating the settling soil, which isn't accurate as the negative skin friction force varies with depth. Fellenius also stated that the negative skin friction (drag load) cannot be accurately calculated using the current conventional methods.

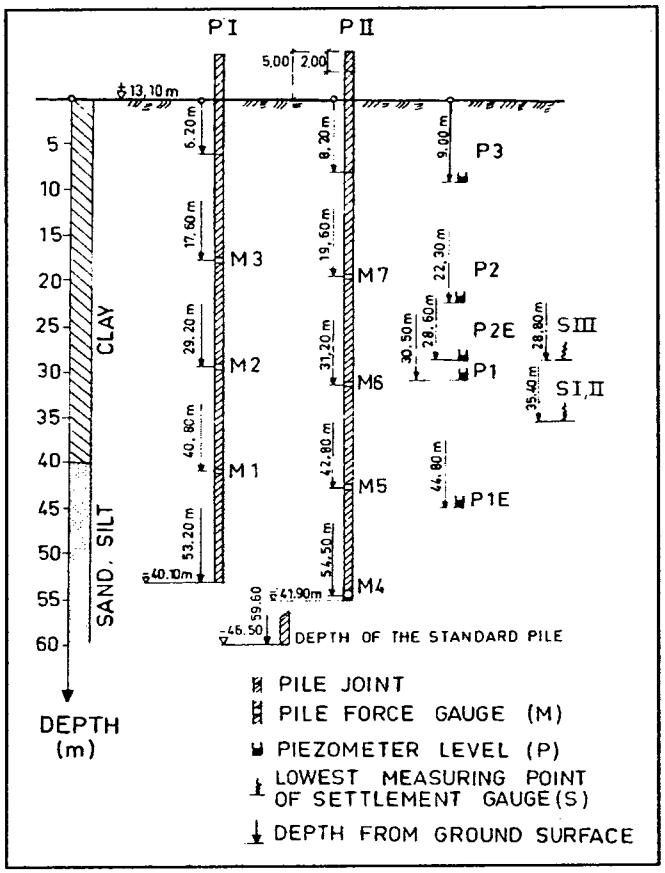

Fig. 2.5 Piles and instrumentation section (Fellenius, 1972)

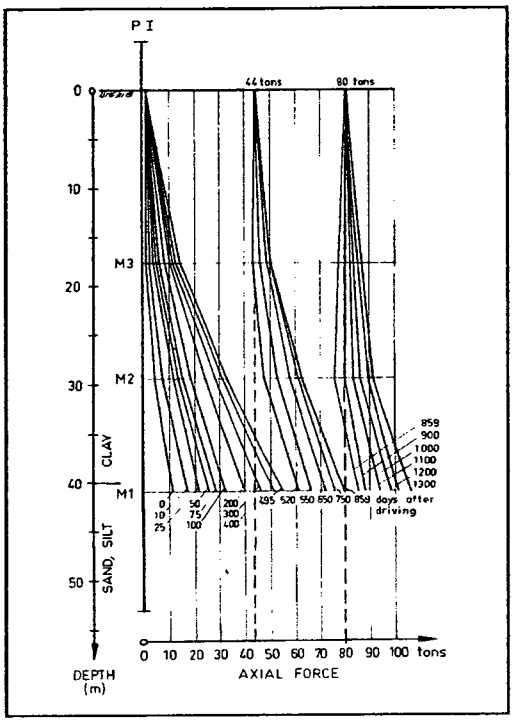

Fig. 2.6 Vertical load distribution in piles PI at various times after the driving (Fellenius, 1972)

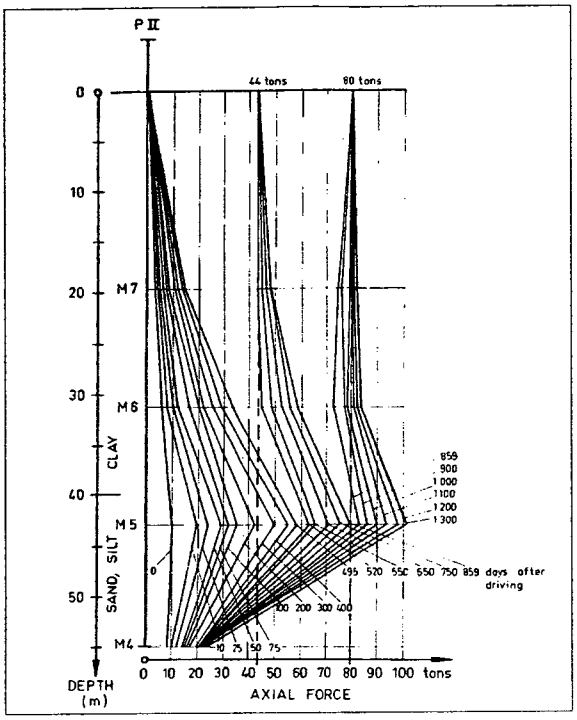

Fig. 2.7 Vertical load distribution in pile PII at various times after the driving (Fellenius, 1972)

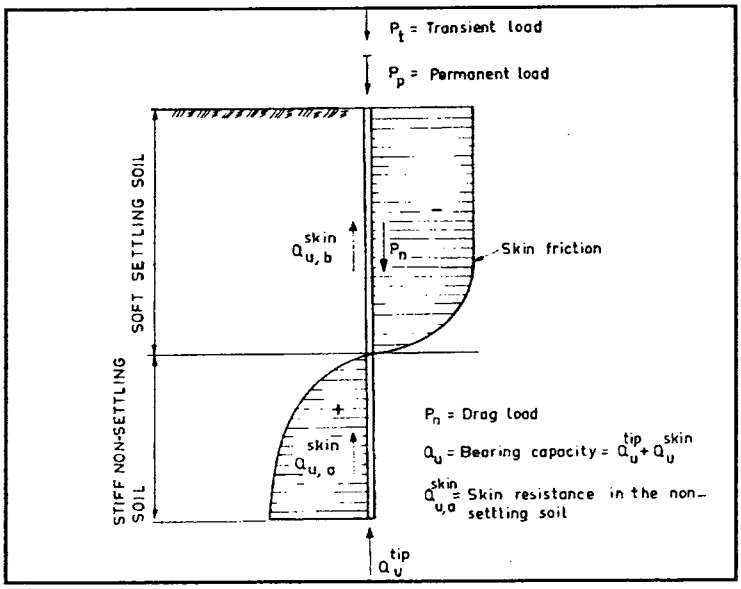

Fig. 2.8 Unit skin friction distribution along a pile in an upper layer of soft settling soil and a lower layer of non-settling soil (Fellenius, 1972)

Meyerhof (1976) states that the problem of negative skin friction is more critical for end-bearing piles rather than floating piles, and that the negative skin friction coefficient β decreases as the pile length increase as shown in figure 2.9, and that in some cases the ultimate skin friction is not mobilized due to the insufficient soil movement.

Ultimate negative skin friction f_s can be calculated from equation [2.3] based on the effective stress σ'_v and β can be calculated from equation [2.4] where, K_s is the ultimate coefficient of earth pressure and φ' is the angle of friction of soil.

$$f_s = \sigma'_v \beta \ldots\ldots\ldots\ldots\ldots\ldots\ldots\ldots \quad [2.3]$$

$$\beta = K_s \tan \varphi' \ldots\ldots\ldots\ldots\ldots\ldots \quad [2.4]$$

Meyerhof has pointed out that the skin friction factor β can vary in a wide range for over consolidated clays with respect to degree of over-consolidation of soil, pile shape, installation method of pile and other factors. Test results have shown that the value of K_s for stiff fissured over-consolidated London clay, can range from 0.7 K_o to 1.2 K_o, and accordingly β varies from 0.7 to 1.4 for bored piles, while for driven piles K_s can range from K_o to more than $2K_o$ accordingly β varies from 1 to more than 2, therefore assuming that K_s is equal to K_o underestimates the skin friction for driven piles and overestimates it for bored piles. Where K_o is the coefficient of earth pressure at rest, can be calculated from equations [2.5] and [2.6] where R_o is the over consolidation ratio of clay.

$$K_o = 1 - \sin \varphi' \ldots\ldots\ldots\ldots\ldots\ldots\ldots\ldots \quad [2.5]$$

$$K_o = (1 - \sin \varphi')\sqrt{Ro} \ldots\ldots\ldots\ldots\ldots\ldots \quad [2.6]$$

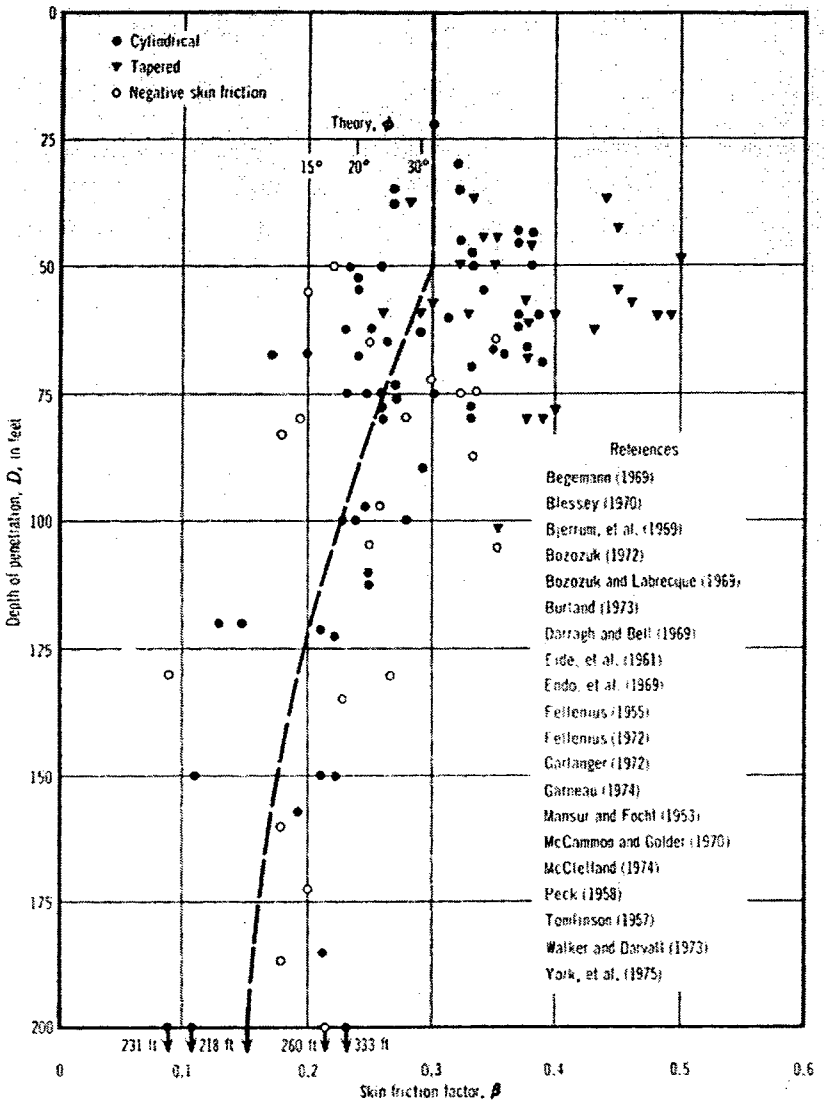

Fig. 2.9 Positive and negative skin friction of driven piles in soft and medium clays (Meyerhof 1976)

Fellenius (1989) reported that the problem of negative skin friction is a problem of settlement and has no effect on bearing capacity, while the allowable load acting on the pile should satisfy both bearing capacity and settlement requirements. He stated also that based on observations for end-bearing piles negative skin friction force can reach very high values. Therefore, for slender end-bearing piles the drag-loads can result in pile

failure if the forces exceed the pile material strength and hence the structural capacity of the pile. Fellenius stated that the results of the field investigations from previous researches show that extremely small movements (as small as 1mm) are large enough to generate negative skin friction force and to reverse the shear-force direction, and since there will always be small movements in soil with time and hence small relative movements between the soil and the pile, therefore all piles are subjected to negative skin friction force, also as a consequence of mobilization of forces along the pile upon extremely small movement, live loads and drag-load should not be added together as they don't act on the pile at the same time.

Fellenius defined the neutral plane as "the depth where the shear stress along the pile changes over from negative skin friction into positive shaft resistance", and he stated that the neutral plane is located where there is no relative movement between the soil and the pile. He states that the location of the neutral plane for piles resting on firm soils bedrock (end-bearing piles) is at the soil-bedrock interface, and for piles resting on less firm soils (floating piles) the neutral plane is below the midpoint of the pile, where the firmer the soil at the pile tip, the lower the neutral plane, and the higher the dead load, the higher the neutral plane as shown in figure 2.11. In case of floating pile in homogenous soil where the applied load is one third the bearing capacity (ie. FS=3), the positive shaft resistance is equal to the negative skin friction and the toe resistance is very small, the neutral plane is located at the lower third of the pile (ie. $0.7L$), which is the same level of the equivalent-footing proposed by Terzaghi and Peck (1948).

Understanding these concepts regarding the neutral plane is essential for studying negative skin friction. Figure 2.10 Shows the distribution of forces along the pile and the location of neutral plane, where:

Q_d = Dead Load

Q_l = Live Load

Q_q = Allowable load = $Q_d + Q_l$

Q_u = Ultimate resistance = R_u

q_n = Unit negative skin friction

Q_n = Accumulated q_n

r_s = Unit positive shaft resistance

R_s = Total shaft resistance

R_t = Toe resistance

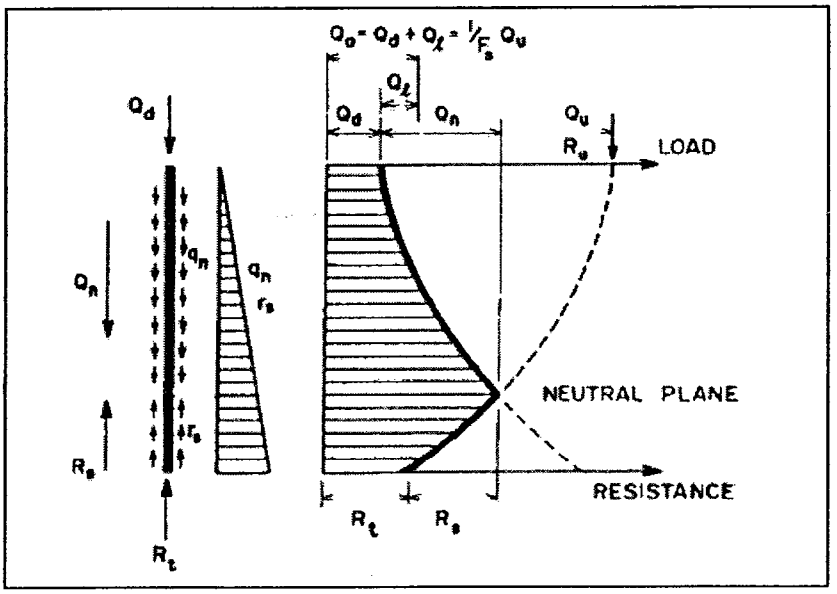

Fig.2.10 Definition and construction of the neutral plane (Fellenius, 1989)

Since the neutral plane is the point where there is no relative movement between the soil and the pile, therefore the settlement of the pile head is equal to the settlement of the soil at the neutral plane added to the elastic compression in pile material due to deadload and dragload together.

The approach suggested by Fellenius can be applied to all types of piles regardless the soil type, settlement magnitude, weather the pile is end-bearing or floating and other different aspects.

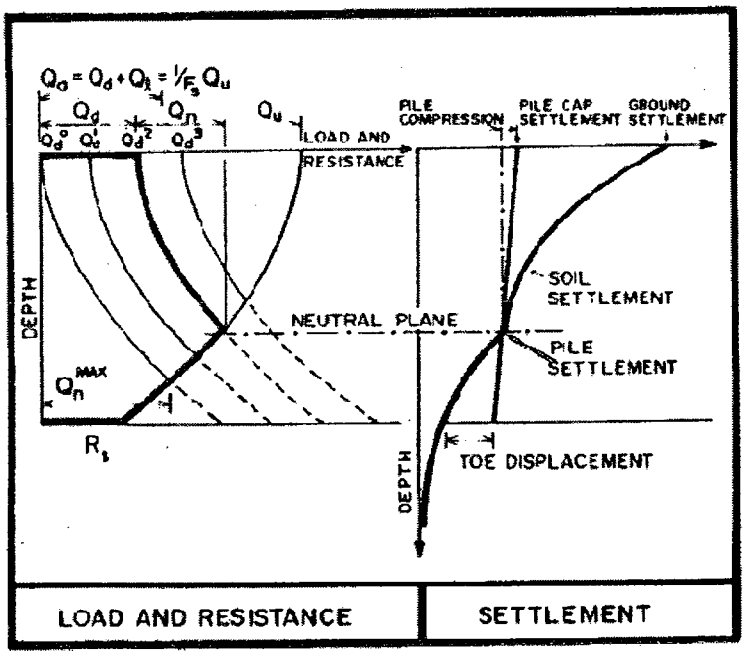

Fig.2.11 Unified design for capacity, negative skin friction, and settlement (Fellenius, 1989)

The suggested design approach consists of four steps, first determining the location of neutral plane, then checking that the pile material structural capacity is adequate, then the pile settlement is computed using the equivalent footing concept, and last step is verifying the bearing capacity of the pile.

Burland and Strake (1994) have gathered some values of β from published researches, based on field tests on driven piles, and compared the values of β as shown in Table 2.2.

Table 2.2 β values from published field data (Burland and Strake, 1994)

Type of soil	Range of β	Type of Pile Material	Reference
Low plasticity marine Clay	0.15-0.25	Steel	Johanneson and Bjerrum (1965)
Silty Clay	0.26	Steel	Bjerrum et al. (1969)
Silty Clay	0.2-0.4	Steel	Endo et al. (1969)
Low plasticity marine Clay	0.12-0.2	Steel	Bozozuk (1972)
Silty Clay	0.51	Steel	Walker and Darvall (1973)
Soft clay	0.2-0.25	Steel	Garlanger (1974)
Highly plastic clay	0.26-0.38	Steel	Auvinet and Hanell (1981)
Clayey silt	0.25-0.4	Steel	Keenan and Bozozuk (1985)
Singapore marine clay	0.35	Concrete	Leung et al. (1991)

Lee et al. (2002) have carried out numerical analyses, to study group effect and distribution of negative skin friction forces on piles' shaft. In this study single piles in 2D axi-symmetrical conditions were studied as well as pile groups in 3D, using the finite element package ABAQUS.

The ABAQUS interface modeling technique was used to simulate the behavior at the pile-soil interface, where the coulomb frictional law is applied to represent the interface frictional behavior.

The study marked the importance of soil slip at the pile-soil interface to be considered to provide an economic solution as the previous elastic solutions in general over-predict the negative skin friction force acting on piles.

In this study the neutral plane for friction piles was located around a depth of 70% of the pile length, measured from the top of the pile, while for end-bearing piles the negative skin friction force acts along the entire pile length, as presented in figure 2.12.

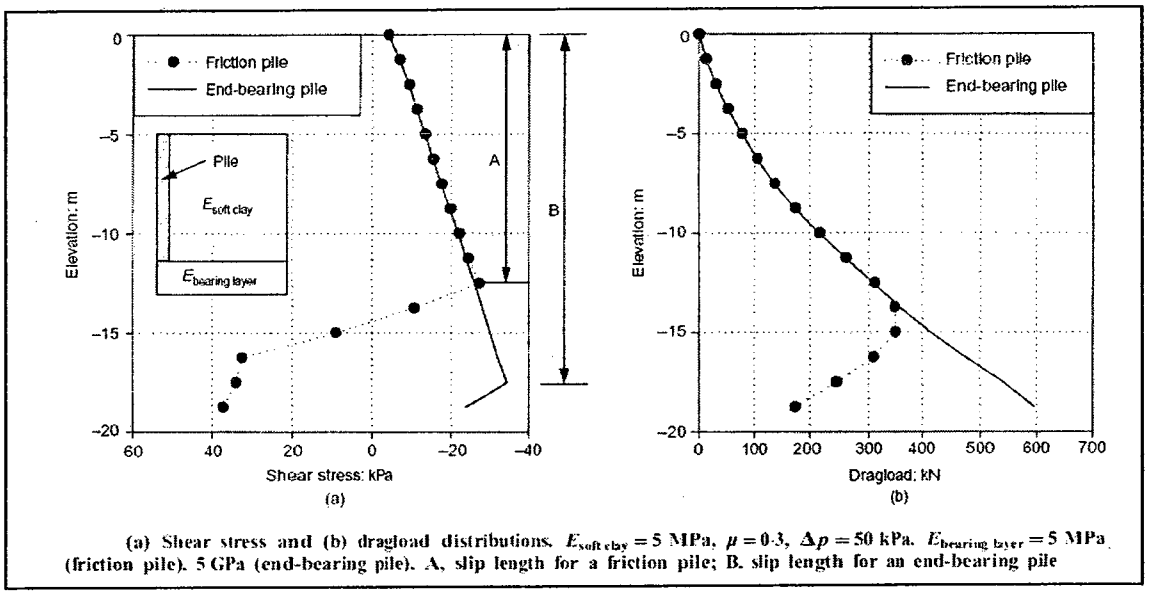

(a) Shear stress and (b) dragload distributions. $E_{soft\ clay} = 5$ MPa, $\mu = 0.3$, $\Delta p = 50$ kPa. $E_{bearing\ layer} = 5$ MPa (friction pile), 5 GPa (end-bearing pile). A, slip length for a friction pile; B, slip length for an end-bearing pile

Fig. 2.12 Shear stress and dragload distributions with respect to depth (Lee et al., 2002)

Hanna and Sharif (2006) have studied the drag force on single piles in clay subjected to surcharge and have established a numerical model using finite element method to predict the pile capacity, factor of safety, neutral plane location and the effect of pile coating.

For floating piles, the negative skin friction acts along the pile shaft till the depth of neutral plane L_{NP}, therefore the equation used for calculating negative skin friction force on floating pile using the beta method is:

$$Q_n = \int_0^{L_{NP}} \beta(\pi D)(\gamma' Z + S)\, dz \ldots\ldots\ldots \quad [2.7]$$

$$\beta = K_S \tan \delta' \ldots\ldots\ldots\ldots\ldots\ldots\ldots\ldots\ldots\ldots \quad [2.8]$$

While in case of end-bearing piles the negative skin friction force acts on the entire pile length (in case of settlement of the whole soft layer), therefore the equation for the end-bearing piles is:

$$Q_{n(max)} = \int_0^{L} \beta(\pi D)(\gamma' Z + S)\, dz \ldots\ldots \quad [2.9]$$

A reduction factor R_N for floating pile was introduced, where R_N is the ratio between the existing or the mobilized negative skin friction force Q_n acting on the pile till the depth of the neutral plane, and the maximum negative skin friction force $Q_{n(max)}$ is the negative skin friction force calculated for the entire pile length.

$$R_N = \frac{Q_n}{Q_{n(max)}} = \left(\frac{L_{NP}}{L}\right)^2 \ldots\ldots\ldots\ldots\ldots\ldots\ldots\ldots\ldots\ldots \quad [2.10]$$

For calculating the working load on the pile or the allowable bearing capacity for pile Q_a is calculated from equation [2.11].

$$Q_a = \left[\frac{Q_t + Q_s}{FS} - Q_n\right] = \left[\frac{Q_t + Q_s}{FS} - R_N Q_{n(max)}\right] \ldots\ldots \quad [2.11]$$

Taking into account the effect of bitumen coating of pile, the value of the coefficient of friction β is reduced, therefore β_c is used for calculating the negative skin friction force

for coated piles instead of β, and the correction factor R_N is calculated from the following equation:

Figures were introduced for obtaining the value of R_N as shown in figures 2.13 and 2.14 for a wide range of parameters namely (N_s, L/D, and FS), where N_s is the surcharge factor, — and for coated piles it was assumed that (β_c=0.05) and (β=0.25).

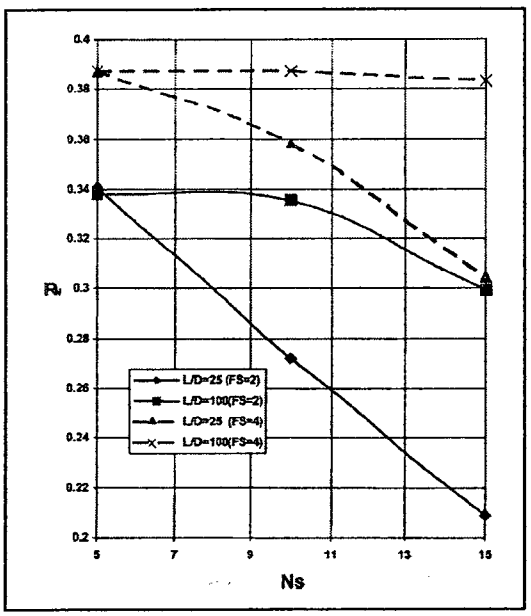

Fig. 2.13 Values of Coefficient R_N for uncoated piles (Hanna and Sharif, 2006)

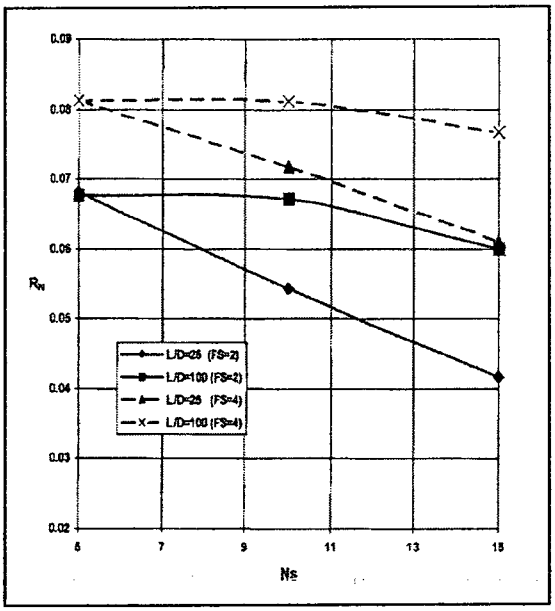

Fig. 2.14 Values of Coefficient R_N for coated piles (Hanna and Sharif, 2006)

Where:

$Q_{n(max)}$: Maximum negative skin friction force

β =coefficient of friction for the pile/clay

Ks: coefficient of earth pressure

δ': angle of friction between soil and pile shaft, taken: (0.5 to 0.7) φ'

Z: Height of fill

S: surcharge pressure

D: Diameter of pile

L: Length of pile penetrating settling soil

L_{NP} : Depth of the neutral plane

Q_t : Ultimate tip resistance of the pile

Q_s : Ultimate shaft resistance of the pile

Q_a : The allowable bearing capacity of the pile

β_c : Coefficient of friction for coated pile–clay material.

Ns: Surcharge factor

In this study the authors reported that under the ultimate load and due to the excessive pile settlement, the negative skin friction force is no longer acting on the pile, while under the working load, negative skin friction force is present, as skin friction force develops when there is a relative movement between soil and pile.

2.4. Problem of Negative Skin Friction on Pile Foundations in Collapsible Soils

2.4.1. General

Negative skin friction force caused by collapsible soil settlement upon wetting is being controlled by many different factors, which makes the problem of negative skin friction on piles penetrating collapsible soils very complex.

The movement in collapsible soil happens suddenly when soil is being wetted (takes place over very short periods) and it can reach a very high magnitude, unlike the consolidation movement in clay which takes place over longer periods of time and of relatively smaller magnitudes. Therefore the negative skin friction forces in collapsible soils are more critical and of higher values than that in clay or other types of soft deformable soils, and accordingly the classic methods for calculating negative skin friction for clay and other soft soils is not sufficient nor reliable for collapsible soil as it underestimates the value of negative skin friction force.

2.4.2. Literature Review Pertinent to Negative Skin Friction on Pile Foundations in Collapsible Soils

Grigoryan and Grigoryan (1975) have carried out for the first time an experimental study on negative skin friction forces on floating piles in collapsible soils.

This study was aimed at studying the effect of collapsible soil on piles upon soil collapse under it's own weight when being soaked with water.

Two bored cast-in-situ testing piles (NI and NII) were installed and equipped with strain gauges to measure the pile movement in the vertical direction and dynamometers (N1 through N6) to measure the forces along the pile shafts as shown in figure 2.15 the dynamometers were installed at different depths. The testing piles NI and NII were of lengths 16 and 22 m and diameters 600 and 500 mm respectively as shown in figure 2.16. Four piles (NIII through NVI) were installed to attain the reaction of the loading jack, and depth markers (D1 through D6) were installed for monitoring soil movement. Figure 2.16 shows the plan view for the piles and depth markers.

Piles were loaded with a constant static load all over the test; and in order to introduce water and soak the soil, trenches have been constructed to be filled with water during the test.

After water was introduced to the soil, soil settlement was observed and negative skin friction forces developed along the pile shaft, as shown in figure 2.17. Where Q is the water discharge, T is the longitudinal forces in piles as measured by dynamometers 1, 4, 5 and 6. And S is the settlements of the piles (NI through NVI) and depth markers (D1 through D6).

Negative skin friction forces only develop when there is a relative movement between soil mass and the pile, i.e. The rate of soil settlement was greater than the rate of the pile settlement, therefore a relationship between the rate of soil settlement and the rate of pile settlement was conducted as shown in figure 2.17 where $\delta s_{so}/\ \delta t$ is the rate of soil settlement while $\delta s_{pi}/\ \delta t$ is the rate of pile settlement, thus negative skin friction occur only when $\delta s_{so}/\ \delta t$ is greater than $\delta s_{pi}/\ \delta t$.

The investigation has shown that there is a relationship between settlement of soil under its own weight upon wetting and negative skin friction forces acting on pile penetrating such soils.

Settlement of piles (downdrag) has been observed only after the soil has started to settle upon wetting.

The negative skin friction forces increase with the increase of relative movement between soil and pile, as shown figure 2.18 and the maximum value of negative skin friction force observed during the test was 282kN.

The pile settlement occurs as a result of a combination of forces subjected to the pile from the super-structure and negative skin friction forces.

The test was conducted for floating piles that experienced settlement, thus the negative skin friction force was developed only due to the small relative movement between soil mass and the pile, where the negative skin friction force acts only till the depth of the neutral plane.

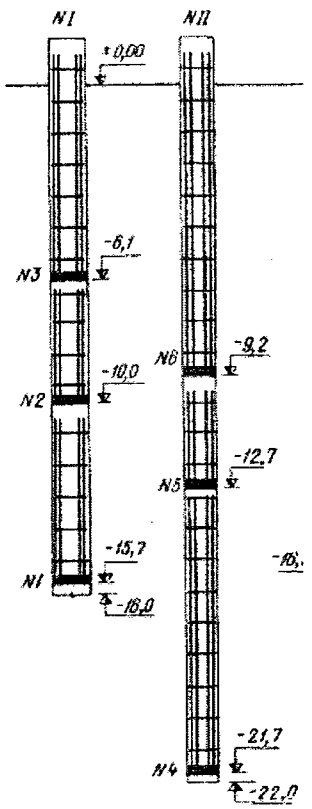

Figure 2.15 Locations of dynamometers along the pile length (Grigoryan and Grigoryan, 1975)

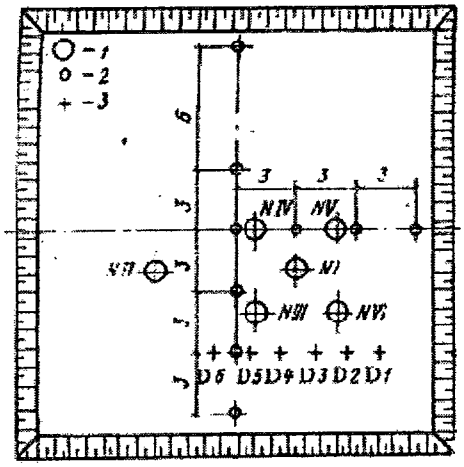

Figure 2.16 Piles and depth markers location (Grigoryan and Grigoryan,1975)

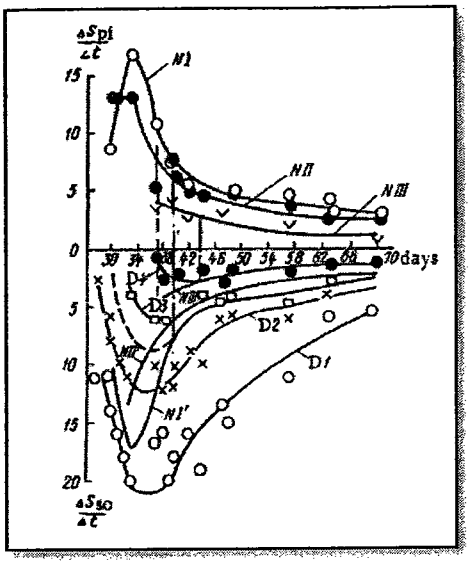

Figure 2.17 Rate of soil and pile settlement (Grigoryan and Grigoryan, 1975)

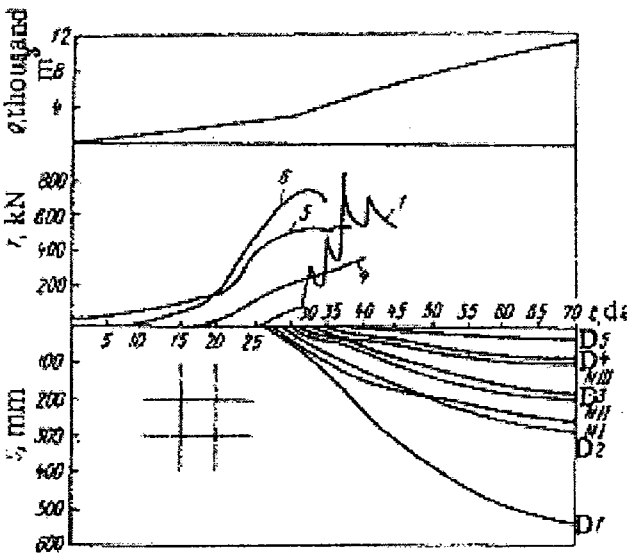

Figure 2.18 The change in time (from the start of slumping) of the rates of settlement of piles and depth marks (Grigoryan and Grigoryan, 1975)

Kalashnikova (1976) has investigated the behavior of floating piles in a collapsible soil stabilized through a leading hole. As the bearing capacity of piles in collapsible soil decrease upon soil wetting; this decrease in strength could be reduced or eliminated by means of soil stabilization using sodium silicate grout. Here we note an experimental investigation comparing the behavior of a pile in a non-stabilized collapsible soil to that of a pile in a stabilized collapsible soil, as shown in figure 2.19.

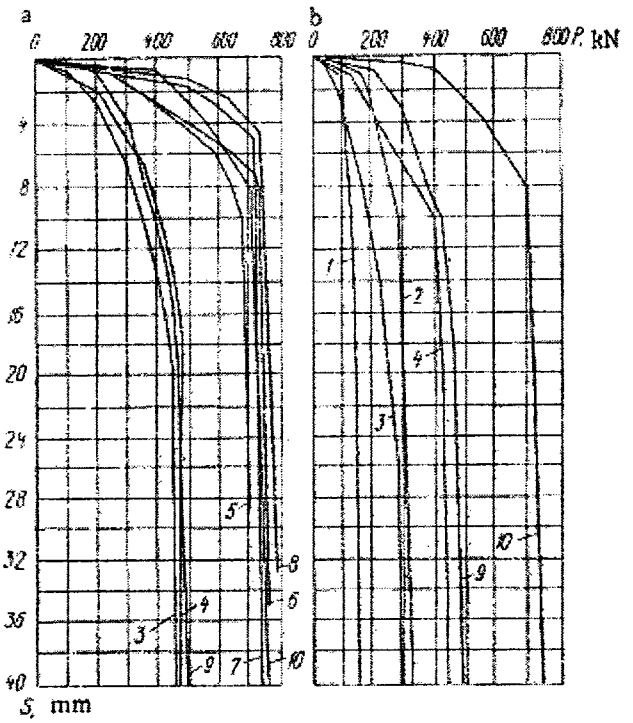

a) Non-stabilized and stabilized piles and pile-plates; b) for separate operation of pile-plates. 1) On lateral surface of SSh-1; 2) the same, for SSh-2; 3) on tip of SSh-1; 4) the same, for SSh-2. No. 9) For joint operation of the tip and lateral surface of SSh-1; No. 10) the same, for SSh-2.

Fig. 2.19 Results of static tests (Kalashnikova, 1976)

The results of the experimental investigation showed that the soil stabilization through a leading hole using sodium silicate grout is an efficient way as the results show that the bearing capacity of piles in stabilized-collapsible soils has increased significantly (50-65%) and accordingly, the settlement has reduced.

Grigoryan (1986) has examined the interaction of cast-in-place piles with soils under type 2 collapsibility conditions.

Investigations were carried out in this study for an existing structure of pile foundation that has been experiencing settlement as the collapsible soil layers are being soaked from top as a result of water leakage from water pipes near by the structure.

For carrying out the testing, strain-gauge piles were installed equipped with dynamometers with pressure transducers of hydraulic type at different depths along the pile length, to obtain strain and stress readings for the testing piles.

Strain-gauge piles are of different lengths resting on hard clay layer for longer piles and collapsible soils for shorter piles.

Strain-gauge piles aren't subjected to any external loads, thus the settlement is caused only by the soil-pile interaction.

Piles carrying the existing structure experienced settlement equivalent to that of the strain-gauge piles throughout the same interval of time.

Not only did the collapsible soil layers settled but the non-collapsible soil layer settled as well.

Both settlement of soil and that of the piles were found to be equal in magnitude and rate, except for the longer piles resting on non-collapsible clay layer, where pile settles more than the non-collapsible clay layer, and negative skin friction force hasn't occurred in any of the two cases.

For longer piles resting on non-collapsible layers settlement remains practically unchanged as pile settlement was equivalent to collapsible layers settlement.

Grigoryan and Chinenkov (1990) have carried out investigations on under-reamed long piles having length to diameter ratio greater than 20, in type 2 collapsible soil on 3 different sites, in order to study the effect of base enlargement on pile bearing capacity and settlement in such soils. For the 3 sites, piles were resting on insufficiently dense soils.

Comparison between settlement of under-reamed piles and similar piles of constant diameter has shown practically that the enlarging in diameter has no significant effect.

For the 3 sites prolonged soil soaking was caused by leakage of water from water conveying pipelines and partial inundation from city side.

The study has proven the non-effectiveness of under-reamed long piles penetrating type 2 collapsible soils and resting on relatively weak strata, and that illustrates that the contribution of the tip resistance to the total pile bearing capacity is very small.

The study has also proven that the increase in the settlement of bored-cast-in-place piles in similar soil conditions are governed by soil settlement conditions under long-term soaking and doesn't depend on the external loads applied on the pile.

Grigoryan (1991) has stated that during the last few years of the late 1980s, a large number of problems in pile foundations have been published. One cause of these problems is due to the effect of negative skin friction on pile bearing capacity and the other is due to the rise in ground water level causing pile foundation settlement.

Grigoryan has proposed three analytical schemes for pile-soil interaction for floating piles penetrating a large layer of collapsible soil as shown in figure 2.20 where S_1 is the soil settlement and S_2 is pile settlement.

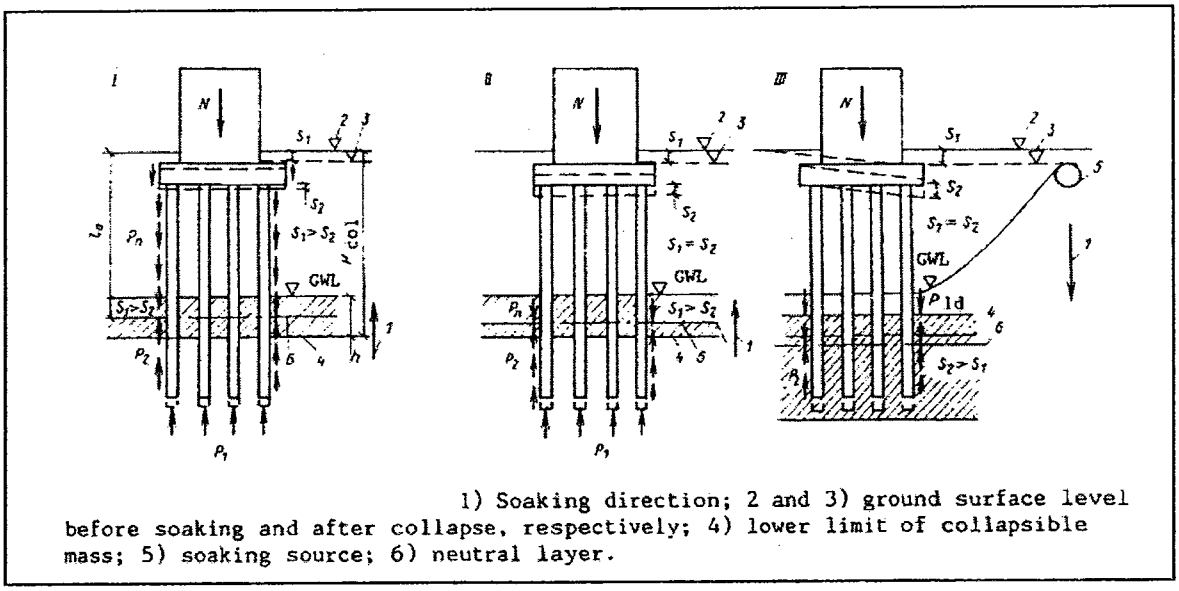

Fig. 2.20 Analytical schemes for pile-soil interaction for floating piles penetrating a large layer of collapsible soil (Grigoryan, 1991)

Grigoryan has listed that it's necessary to conduct a method for predicting pile settlement in loess soils instead of using the approach of decreasing the pile bearing capacity.

Practical observations were made for tens of projects confirming the third scheme in the figure, but the first and second ones, haven't been confirmed by practical observations in construction practice.

Grigoryan has proposed measures for eliminating settlement of pile foundations in collapsible soils as follows:

1. Construction of deep piles resting on firm strata.
2. Eliminating the possibility of soaking soils entirely.

And both measures are highly uneconomical solutions as Grigoryan lists.

Krutov (2003) has investigated negative skin friction forces acting on piles penetrating collapsible soils, and suggested an approach to be carried out to take into account negative skin friction when designing piles in collapsible soils.

Krutov listed that there is lack of complete consideration of additional loads applies by collapsing soil masses known as negative skin friction forces, and that there are many factors that should be considered, such as: Characteristics of collapse, compressions of soils underlying collapsible soils, the thickness of collapsible soil layer, the type and location of sources of wetting, the pattern of soil-pile interaction, along with other factors.

He suggests different schemes for soil-pile interaction depending on the stiffness of soil layers underlying the collapsible soil layer as shown in figure 2.21.

Previous experimental investigation shows that an additional load on the pile (negative skin friction force) appeared simultaneously with the settlement of soil under its own weight upon wetting.

The study proposes some additional factors to be considered for the design of pile foundations in collapsible soils collapsing under its own weight upon wetting.

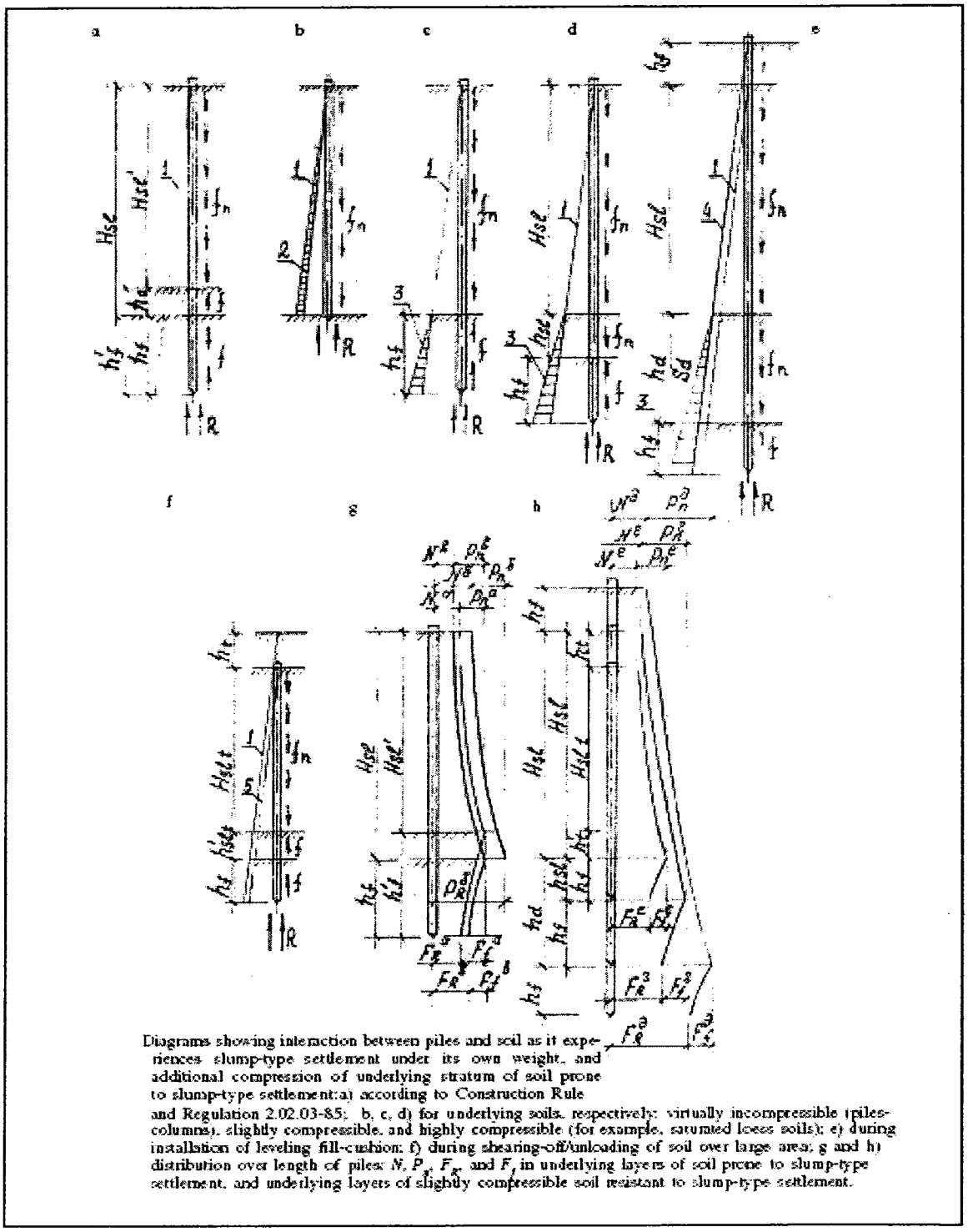

Diagrams showing interaction between piles and soil as it experiences slump-type settlement under its own weight, and additional compression of underlying stratum of soil prone to slump-type settlement:a) according to Construction Rule and Regulation 2.02.03-85; b, c, d) for underlying soils, respectively: virtually incompressible (piles-columns), slightly compressible, and highly compressible (for example, saturated loess soils); e) during installation of leveling fill-cushion; f) during shearing-off/unloading of soil over large area; g and h) distribution over length of piles N, P_n, F_R, and F_f in underlying layers of soil prone to slump-type settlement, and underlying layers of slightly compressible soil resistant to slump-type settlement.

Fig. 2.21 Interaction between piles and soil subjected to collapse settlement under its own weight (Krutov, 2003)

Grigoryan (2005) has analyzed Krutov's paper with disagreement in many points.

He lists that although pile foundations in collapsible soils were used widely in the 1960s, and multiyear study for this problem was carried out in Russia, however it didn't reflect on the Russian construction code of practice for pile foundations.

The author mentions that the study carried out by (Krutov 2003), inadequately account the additional negative skin friction forces due to soil settlement under its own weight upon wetting and the additional settlement of compressible soil layers underlying the collapsible soil layer.

There are different complex factors affecting the stress-strain relationship in pile-soil system that haven't been considered by (Krutov 2003) as well.

The Design bearing capacity value obtained by the equation in the Russian construction code of practice for pile foundations is insufficient and in some cases results in "negative" value for bearing capacity which is impossible. The factors suggested by (Krutov 2003) result further reduction for the bearing capacity value, which is unacceptable.

The consideration of time factor is very important, and since the rate of rise in GWT doesn't exceed 0.5-1.5m/year for collapsible soils, therefore settlement may take place over months, so the case of soaking due to rise in GWT might not be critical.

Gao, et al. (2007) have conducted a static load test on a special type of pile (squeezed branch and plate pile) in collapsible soil to investigate the load transfer mechanism.

It is one of the latest studies on piles in collapsible soil; however it focuses only on the effect of using the squeezed branch and plate pile, comparing it to ordinary piles with constant diameter.

Squeezed branch and plate piles are piles of variable diameters, having enlargements along the pile shaft as shown in figure 2.22.

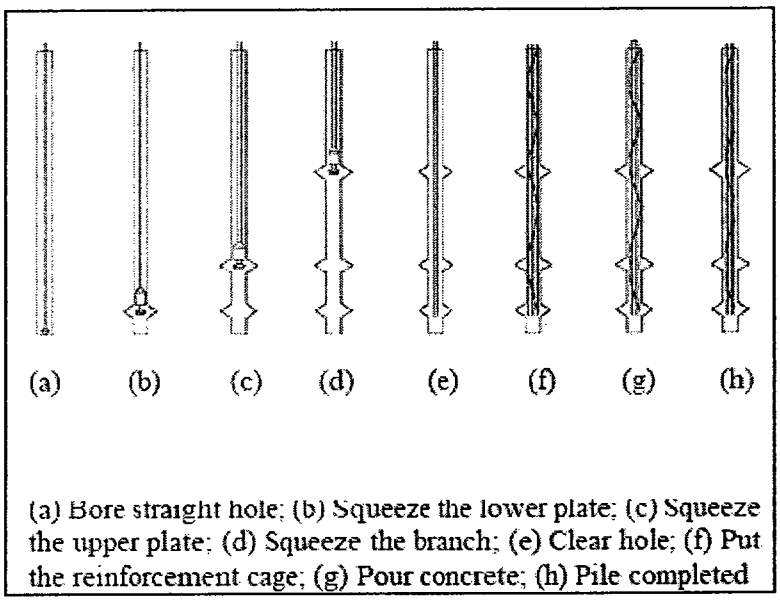

Fig.2.22 Sketch of construction progress of squeezed branch and plate pile (Gao, et al. 2007)

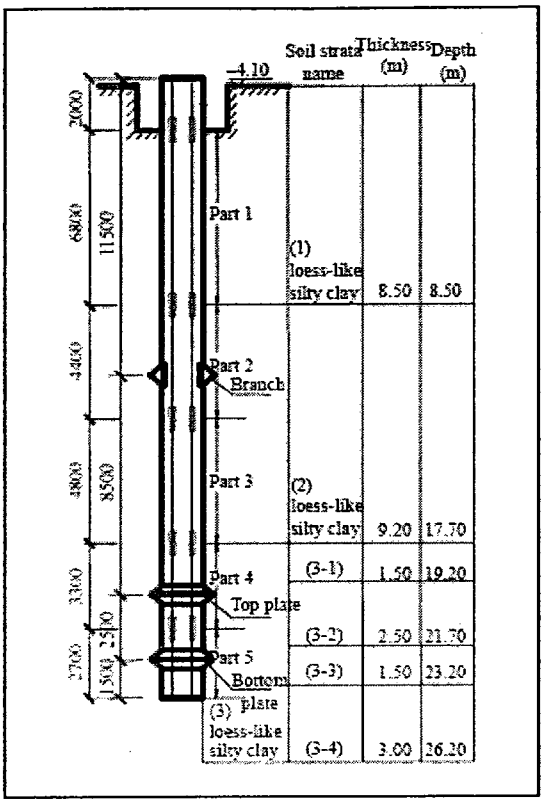

Fig. 2.23 Position of stress gauges, (Gao, et al. 2007)

In this study load transfer mechanism, the ultimate bearing capacity and settlement of squeezed branch and plate pile in self-weight collapsible soil was studied through an experimental model. Stress gauges were installed to monitor the stress along the pile length as show in fig.2.23 as the load transfer mechanism for squeezed branch and plate pile is very complicated. The soil was pre-wetted before carrying out the test, to eliminate the soil settlement, and as a result the effect of negative skin friction hasn't appeared.

The study shows the load mechanism and contribution of skin resistance and toe resistance of squeezed branch and plate piles in pre-wetted collapsible soils, and it shows that the load transferred to the toe was very low, while the bigger portion of the load was carried by branch and plate.

In this study the effect of negative skin friction didn't appear, however the author empathized the importance of examining negative skin friction forces acting on piles in collapsible soils.

2.4.3 Discussion

The review of the literature revealed that the classic methods for calculating negative skin friction on pile foundations cannot be applied for case of collapsible soil, therefore further study should be conducted taking into account the complexity of the problem stated.

2.5. Research Objectives

1. To conduct an experimental investigation on negative skin friction on piles penetrating collapsible soils.
2. To develop an analytical mode to calculate negative skin friction force on piles in collapsible soil based on experimental results.
3. To develop design procedure and design charts for practicing use for piles in collapsible soils.
4. To recommend on future research work on the subject matter.

CHAPTER 3

EXPERIMENTAL INVESTIGATION

3.1. General

In this chapter, the material used in this investigation was first tested to determine its properties. The design of the experimental setup is presented followed by the test procedure.

3.2. Soil Mixtures Preparation

Three different mixtures of collapsible soil were designed and used in the experiments, in order to reach different levels of collapse potential. The mixtures consist of sand and Kaolin with different clay content values and water content of 5%, as shown in table 3.1. The different soil characteristics were determined through a series of soil properties tests, as presented in this chapter.

3.2.1. Determining Different Soil Properties

Sieve analysis was carried out for the soil mixtures to plot the grain size distribution and determine the soil types as summarized in table 3.1.

From sieve analysis and grain size distribution curves, the diameters corresponding to percentage of soil passing sieves D_{10}, D_{30} and D_{60} were determined and the coefficient of curvature C_c and The uniformity coefficient C_u were calculated, where $C_c = D^2_{30}/D_{60}*D_{10}$ and $C_u = D_{60}/D_{10}$.

Classification of soils according to USCS and AASHTO were presented as shown in table 3.1.

The clay material used in the soil mixtures is kaolin, acting as the cementing material that bonds soil particles together, where water is being added in a low percentage of 5%.

A series of soil tests were carried out to determine the unit weight, dry unit weight and the water content of the soil for each of the three soil mixtures after compaction and just before carrying out the experiments, and the results are summarized in table below.

Table 3.1 Soil physical properties

Parameter / Soil type	Mix. 1	Mix. 2	Mix. 3
Clay Content (% Kaolin)	10	8	6
Unit weight γ (kN/m^3)	16.2	16.25	16.28
Dry Unit weight γ_d (kN/m^3)	15.4	15.5	15.6
Specific Gravity G_s	2.67	2.67	2.66
Void Ratio e	0.70	0.69	0.67
Degree of Saturation S (%)	19.05	19.35	19.77
Initial moist content w_c (%)	5	5	5
L.L.	15.9	N.A.	N.A.
P.L.	13.35	N.A.	N.A.
P.I.	2.55	N.A.	N.A.
C_u	21.9	5.4	4
C_c	6.47	1.65	1.27
Unified Soil Classification System USCS	SP-SM	SP-SM	SP-SM
AASHTO	A-2-4	A-3	A-3

Standard proctor test was carried out on the three soil mixes and the compaction curve was plotted to determine the maximum dry unit weight and the optimum moisture content. Figure 3.1 shows the compaction curves for each of the three soil mixes.

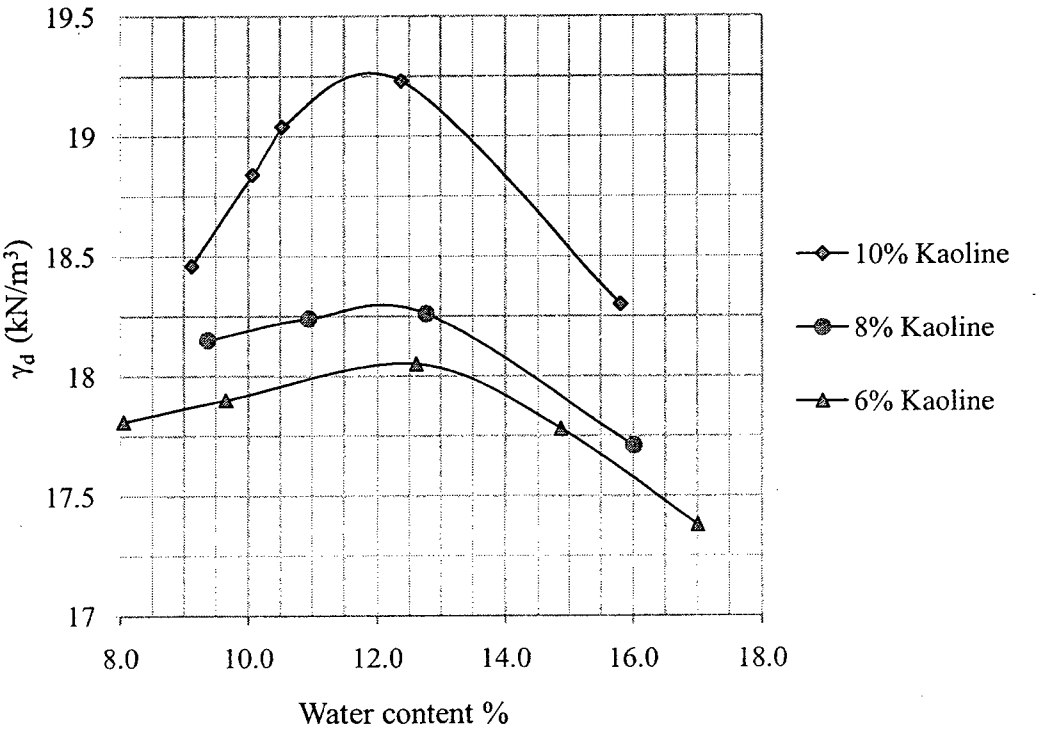

Fig.3.1 Compaction curves for soil mixtures

Table 3.2 Maximum dry density versus optimum moist content

Soil	Max dry unit weight $\gamma_{d\,max}$ (kN/m^3)	Optimum moist content (%)
Soil 1	19.25	11.75
Soil 2	18.3	12
Soil 3	18.1	12.6

3.2.2. Shear Strength Parameters of the Soil Mixture

Direct shear test was performed for each of the three soil mixtures to determine the shear strength parameters. For each soil mixture four direct shear tests were performed at different vertical stresses. The Mohr-Coulomb criterion was used to determine the shear strength parameters of the soil mixture. Table 3.3 presents a summary of these results.

Table 3.3 Summary of shear strength parameters for the soil mixtures

Soil Type	Soil cohesion c' (kPa)	Angle of internal friction φ' (degrees)	Clay Content (%)	Collapse potential C_p (%)
Mix 1	15.5	35	10	12.5
Mix 2	12.5	38.5	8	9
Mix 3	9	40	6	4.2

3.2.3. Collapse Potential C_p of the Soil Mixtures

Oedometer test was carried out on the soil mixes to determine the collapse potential C_p, following the procedure suggested by (Knight 1963) to determine C_P, where the soil specimen is being loaded up to a load of 200kPa, then soil is being flooded with water while the load is maintained on the soil and the settlement upon wetting (collapse settlement) is measured. The e-log p curve is being plotted from the test results and the collapse potential is equal to the deformation of soil due to the addition of water, divided by the initial height of the specimen, expressed in percent as shown in equation [1].

Table 3.4 shows the collapse potential values C_p obtained by oedometer test for each of the soil mixes and the severity of foundation problem as suggested by (Jennings and Knight 1975).

Table 3.4 Collapse potential and severity problem for the soil mixtures

Soil Mixture	Collapse potential (%C_p)	Severity of foundation problem (Jennings and Knight 1975)
Mix. 1	12.5	Severe trouble
Mix. 2	9	Trouble
Mix. 3	4.2	Moderate trouble

3.3. Test Setup

The setup used in the present investigation consists of the following components:

Testing Tank

The testing tank is made of plexi-glass reinforced by aluminum channels and steel angles, providing rigidity for the tank, as shown in figure 3.2.

The inner dimensions of the tank are 50cm width, 50 cm length and 60 cm height.

There are eight pipes connected to the bottom of the tank to allow a uniform distribution of water inflow during the test.

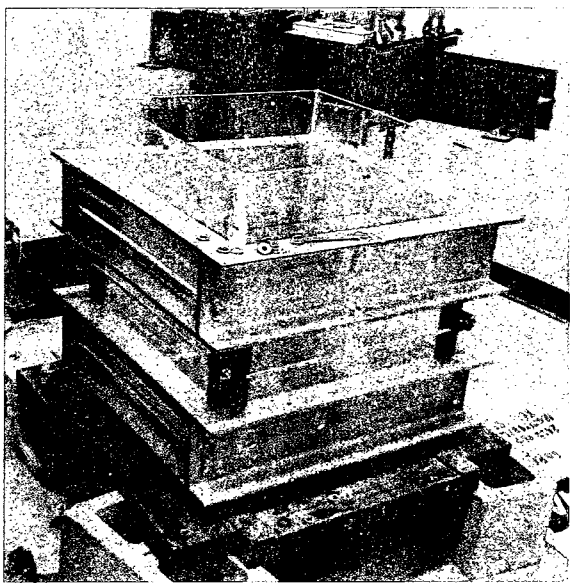

Fig. 3.2 Testing tank

The compaction unit used for compacting soil consists of a hammer of 12.5 kg weight that falls freely from a height of 20 cm and an aluminum plate with an area of 30.5*50 cm^2 with a hole in the middle to allow the pile to pass through as shown in figure 3.3.

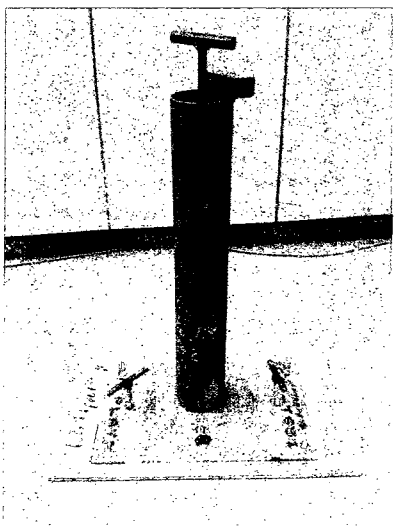

Figure 3.3 Soil compaction unit

Water Supply Unit

The water supply unit consists of a constant-head elevated tank made of plexi-glass and connected to an inflow pipe at the base of the tank to introduce water. An outflow pipe is located at a constant height to drain the excess water in the water tank and maintain a constant water level. A second outflow pipe is connected to the bottom of the water tank to provide water to the testing tank (soil tank) as shown in figure 3.4(a).

The outflow pipe providing water from the elevated tank is connected to a water distributer as shown in figure 3.4 (b). The water distributer provides water to the soil tank through four water-supply pipes that are connected to eight water inlet pipes at the base of the soil tank.

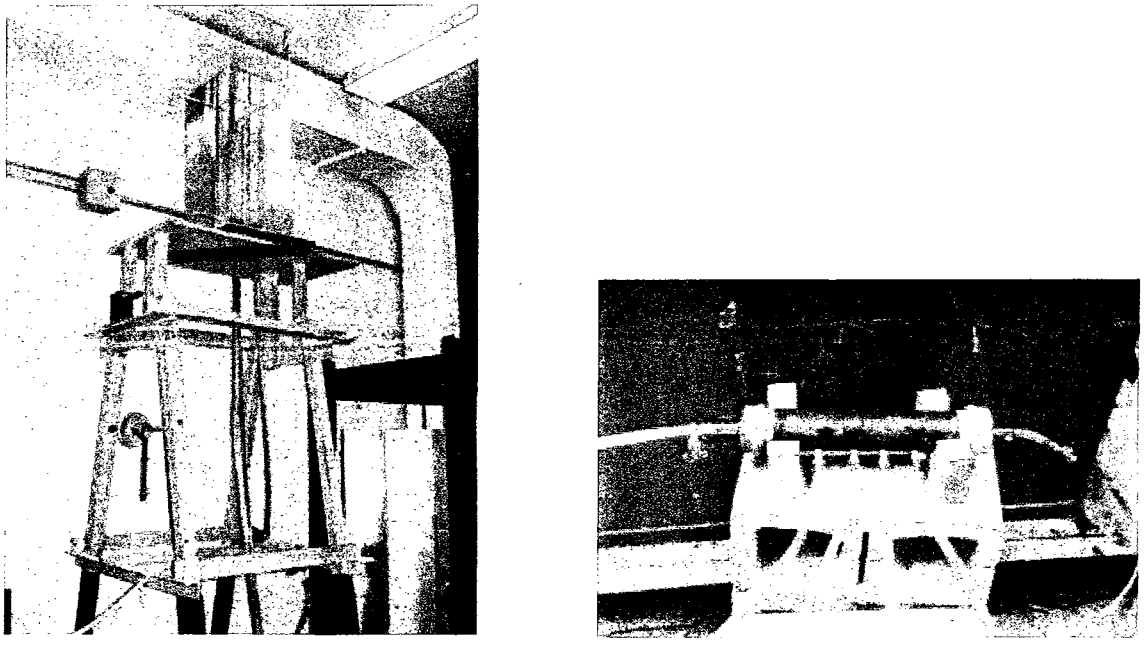

(a) **(b)**

Figure 3.4 (a) Elevated water tank (b) Water-supply pipes

Testing Pile

The testing pile consists of a stainless steel rod diameter of 2.5 cm and a length of 1.5m.

The pile surface for the lower part of the pile (the lower 1.0 m) is a rough surface, in order to insure the interaction between soil and pile due to the friction on pile-soil interface, and the friction of the pile surface for this part is to be assumed as that of steel piles used in practice, while the pile surface for the upper part of the pile (the upper 50 cm) is a smooth surface.

Figure 3.5 shows the difference in pile surface roughness between the lower and the upper parts of the pile.

Figure 3.5 Pile's shaft

Loading Unit

The loading unit was used during the tests to apply stress (surcharge) on soil surface.

The loading unit consists of a loading cylinder that is connected to a hydraulic pump, and a steel plate was used to apply stress from loading unit to the soil surface, with dimensions of 50*50 cm^2, covering all the surface area of the soil, with a circular hole in the centre of the plate of diameter 1 inch to allow the pile to pass through.

Figure 3.6 (a) shows the hydraulic pump, while figure 3.6 (b) shows the hydraulic cylinder connected to a steel beam. Figure 3.7 shows the upper part of the experimental setup, where the steel beam attached to the loading cylinder is fixed to the orange steel frame. The capacity of the loading unit is 11 tonne.

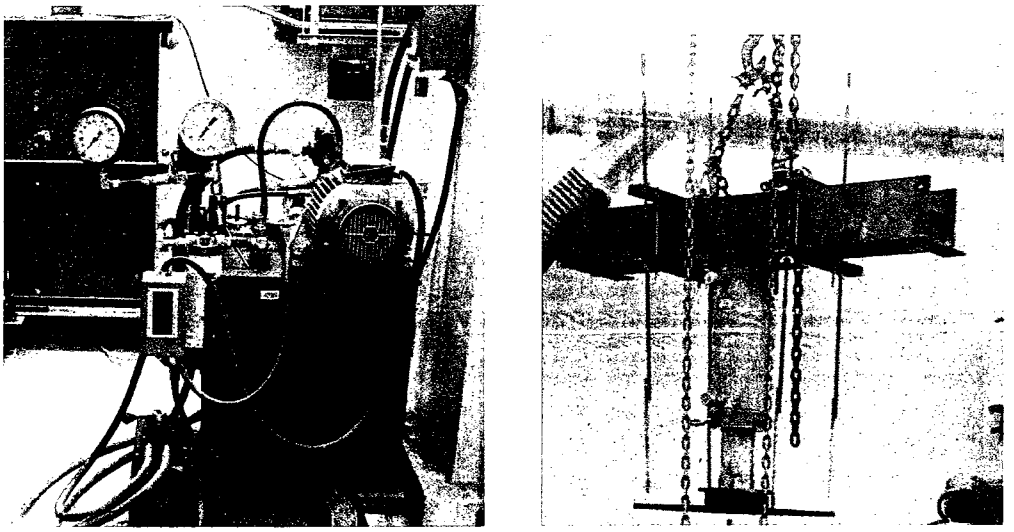

(a) (b)

Figure 3.6 (a) Loading pump (b) Loading cylinder

Loading Lever

A loading lever of 2 tonne capacity was used to apply a static load on pile, in order to insure the full contact between pile and the lower load cell resting on the soil tank bed. The loading lever rests on the upper load cell and the reaction of the lever is transferred to a small beam at the top of the loading lever, as shown in figure 3.7.

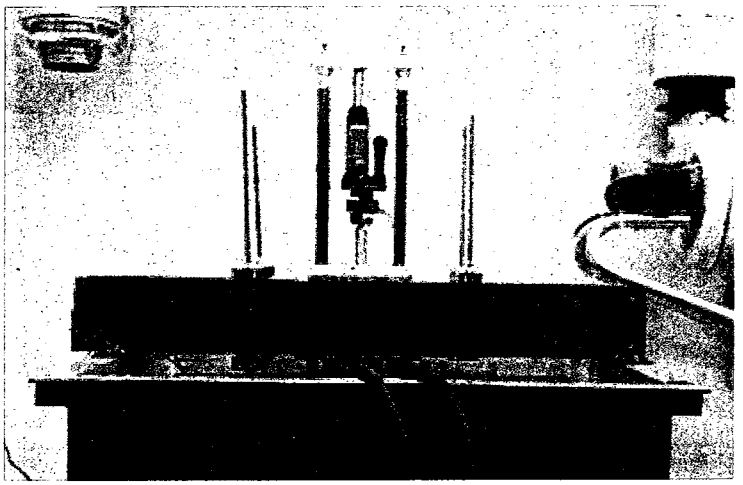

Figure 3.7 Loading lever and steel frame

Load Cells

Two load cells were used during the tests to monitor readings at both the top and the tip of the pile. Figure 3.8 (a) and (b) show the tip load cell attached to the bottom of the pile, while figure 3.8 (c) shows the upper load cell attached to the top of the pile.

Load cells are connected to a voltage unit that introduces an electric current to the load cells and also connected to data acquisition system that is connected to computer, so that all readings are being displayed and monitored on the computer.

The load cells were calibrated and formulae have been developed for each, so that the readings obtained by data acquisition system in volts could be converted into force in Kg.

Both load cells have capacities of 500Kgf.

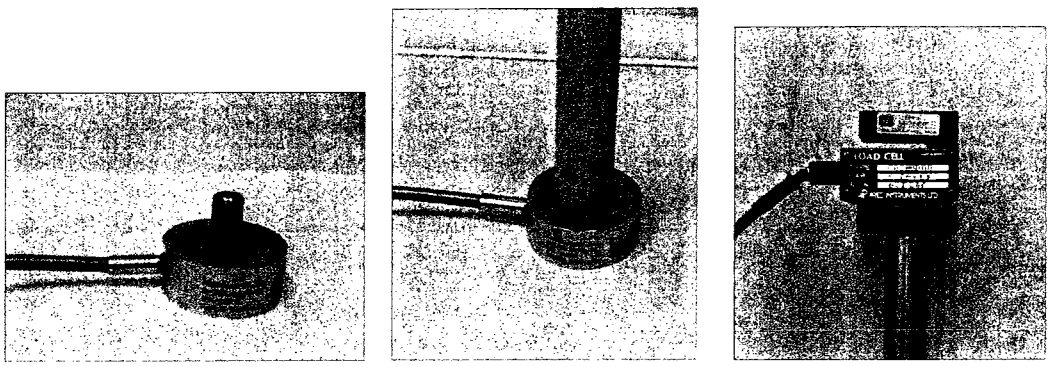

(a) (b) (c)

Fig 3.8 (a) Tip load cell (b) Pile connected to tip load cell (c) Top load cell connected to the pile

Linear Variable Differential Transducers (LVDTs) and Data Acquisition System

Four LVDTs were used to measure the movement of the steel plate and hence the settlement of soil. The LVDTs are connected to a voltage unit that introduces an electric current to LVDTs and also connected to data acquisition system that is connected to computer. The four LVDTs were calibrated and formulae have been developed for each, so that the readings obtained by data acquisition in volts could be converted into millimetres. Figure 3.9 shows the data acquisition system and the LVDTs.

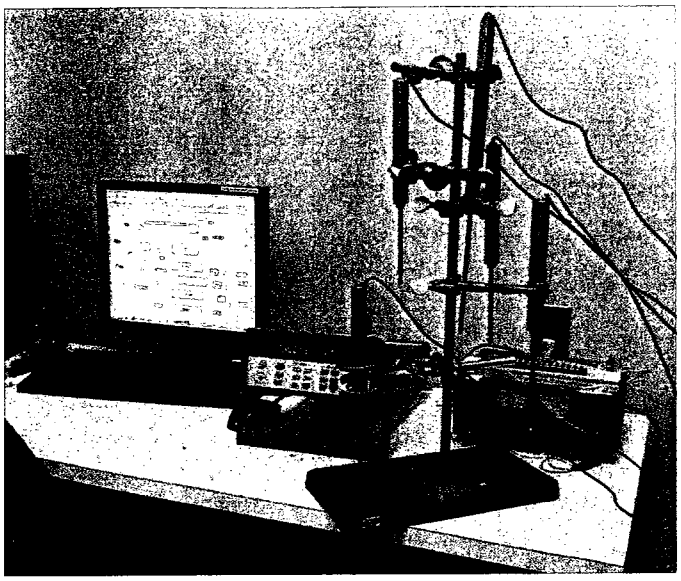

Figure 3.9 Data acquisition system and LVDTS

A special program was developed using VEE pro 8.5 to obtain readings from the four LVDTs and the two load cells in volts and send them to the computer throughout the test in the desired time intervals.

The program was provided with formulae to convert the readings obtained by the LVDTs from volts to millimetres and those obtained by the load cells from volts to kg, using the formulae obtained from calibration of each instrument individually, then send the values obtained from the formulae to an excel sheet that contains readings of four LVDTs in millimetres and readings of the two load cells in kg versus time.

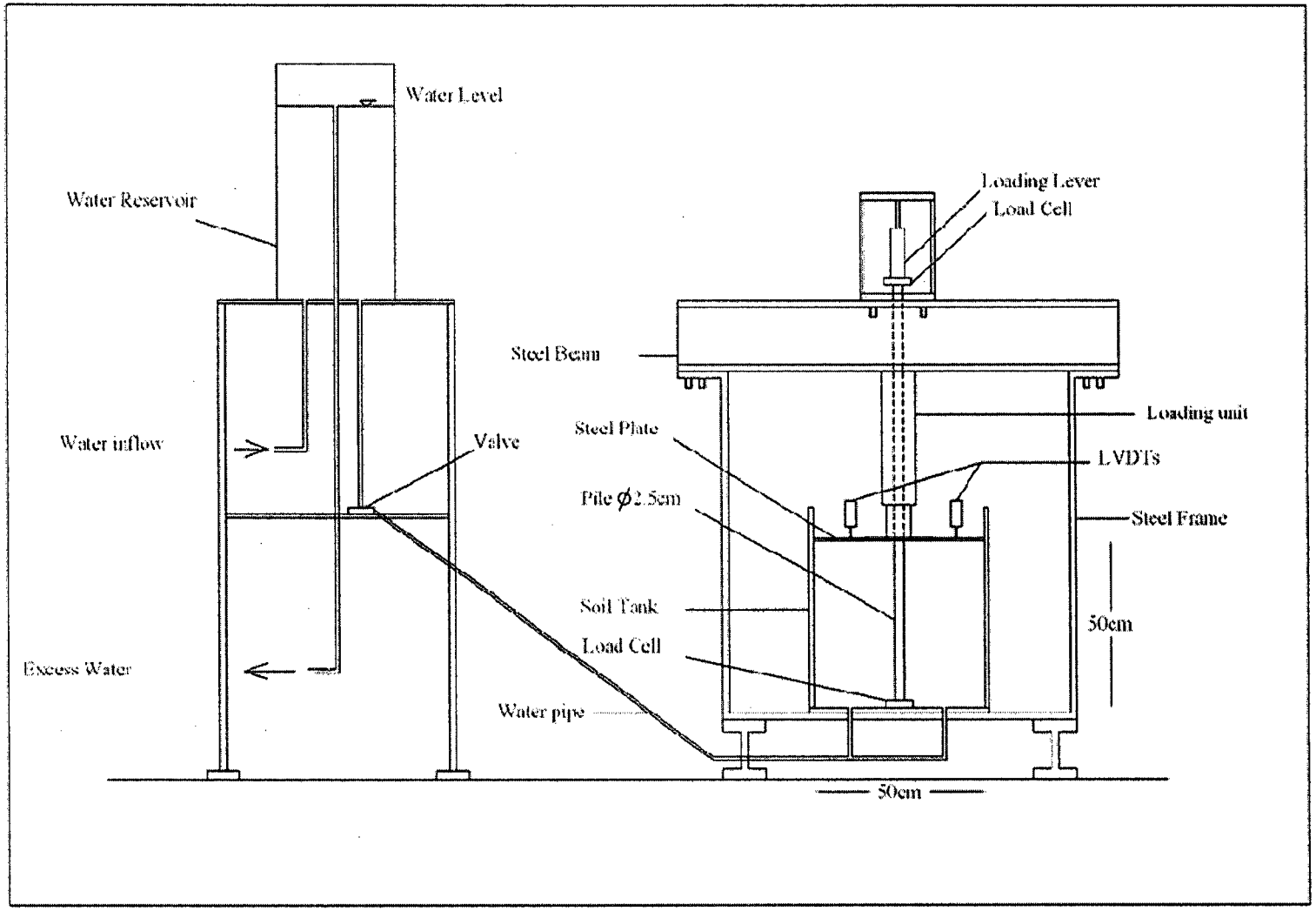

Fig.3.10. Experimental setup

3.4. Experiment Procedure

-Pile is placed in the tank resting on a load cell that is attached to the bottom of the tank, and another load cell is placed one at the top of the pile, as shown in figure 3.10.

-A filter layer 2.5 cm thick of coarse silica sand is placed at the bottom of the tank, so that water infiltrates the soil uniformly.

-Soil is being mixed using a concrete mixer. A sensitive balance was used to maintain the clay percentage for each soil mixture to obtain the desired soil properties summarized in table 3.1.

-After soil has been mixed, soil is placed in the tank on five layers, where soil is being spread then compacted for each layer as shown in figure 3.11. Soil compaction is carried out prior to the loading of soil to reduce void ratio and increase the value of the unit weight of soil. The same compaction energy per unit volume E was maintained for each layer and throughout all the experiments to reach the desired soil properties, and accordingly the desired collapse potential.

Figure 3.11 Soil compaction

It is very important to maintain the energy of compaction to obtain the desired soil parameters and most importantly the desired collapse potential, therefore the compaction energy was calculated and compaction process was carefully carried out throughout the experiments.

Energy of compaction was calculated using this equation:

$$E = \frac{N * W * H * L}{V} \quad \text{[3.1]}$$

Where:

E: Energy per unit volume (gm.cm/cm^3)

N: No. of blows

W: weight (gm)

H: height (cm)

L: no of layers

V: volume of soil being compacted (cm^3)

E ($gm.cm/cm^3$)	N	W (gm)	H (cm)	L	V (cm^3)	V (cm^3)
590.16	36	12500	20	5	50*50*30.5	76250

-Soil samples were taken from the compacted soil prior to carrying out the experiment to determine water content, unit weight, dry unit weight and shear strength parameters.

-Loading plate is placed on the top of soil, connected to a hydraulic loading unit with built-in stress gauges, to allow loading of soil with desired stresses on increments, as shown in figure 3.6.

-Four LVDTs are placed at the top of the loading plate and connected to data acquisition system to monitor the movement of the loading plate and accordingly the soil movement (settlement). Figure 3.12 shows the fixation of the LVDTS during the test.

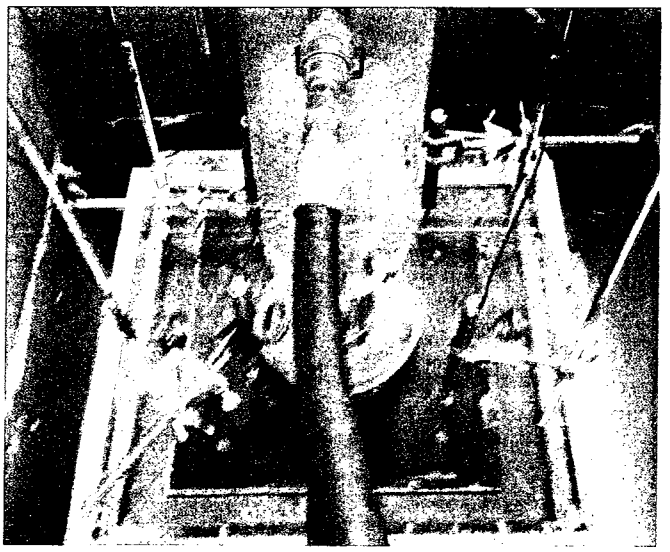

Figure 3.12 LVDTs during the test

-Load is applied to the soil on increments, where stress-controlled loading system was adopted and settlement was monitored until the maximum stress is reached (inundation pressure).

At the inundation pressure, water flow is introduced from downwards to upwards with a constant head, till soil is being 100% inundated.

After Soil is 100% saturated load on soil remains constant for 24 hours.

Static load is applied to the pile constantly throughout the experiment.

The following parameters are being monitored all over the experiment:

-Settlement of soil (LVDTs).

- The surcharge load acting on soil (stress gauges).

-The static load at the top of the pile (load cell on top of the pile).

-The load at the tip of pile (load cell at the bottom of the pile).

CHAPTER 4

RESULTS AND ANALYSIS

4.1. General

In this chapter the testing results are presented in form of tables and figures, showing the behavior of the soil under surcharge load, the effect of wetting on soil under load in terms of settlement, and the negative skin friction subjected to the pile due to soil settlement. Also a series of figures have been conducted showing relationships between different parameters will be used later on in this chapter for illustrating analysis.

4.2. Testing Program

A series of tests were carried out to study the effect of the following:

A- The effect of collapse potential on negative skin friction forces on pile.

B- The effect of inundation pressure on negative skin friction force on pile.

Table 4.1 shows a summary of the different tests, in terms of the different soil mixture types having different collapse potential and inundation pressure. In order to study the effect of the collapse potential on negative skin friction forces on pile tests 1 through 3 were performed, while in order to study the effect of the inundation pressure on negative skin friction force on pile, for the soil mix of high collapse potential, tests 3 through 5 were performed.

Table 4.1 Testing program

Test	Pile Length L (cm)	Pile Diameter D (cm)	Soil Mix.	C_P (%)	Inundation pressure S (kPa)	Clay content (%)	γ (kN/m^3)	γ_d (kN/m^3)	Gs	e	w_c (%)	c' (kPa)	φ'	LL	PL	PI	USCS
Test 1	48	2.5	1	12.5	40	10	16.2	15.4	2.67	0.7	5	15.5	35	15.9	13.35	2.55	SP-SM
Test 2	48	2.5	1	12.5	60	10	16.2	15.4	2.67	0.7	5	15.5	35	15.9	13.35	2.55	SP-SM
Test 3	48	2.5	1	12.5	80	10	16.2	15.4	2.67	0.7	5	15.5	35	15.9	13.35	2.55	SP-SM
Test 4	48	2.5	2	9	80	8	16.25	15.5	2.67	0.69	5	12.5	38.5	N.A	N.A	N.A	SP-SM
Test 5	48	2.5	3	4.2	80	6	16.28	15.6	2.66	0.67	5	9	40	N.A	N.A	N.A	SP-SM

4.3. Testing Results

In the following section, the results obtained from the present experimental investigation were presented in graphical forms.

Test Number 1:

In this test, soil mixture 1 with a high collapse potential C_P equal to 12.5% was used, and the soil was inundated at pressure of 40 kPa, results are shown in the figure below

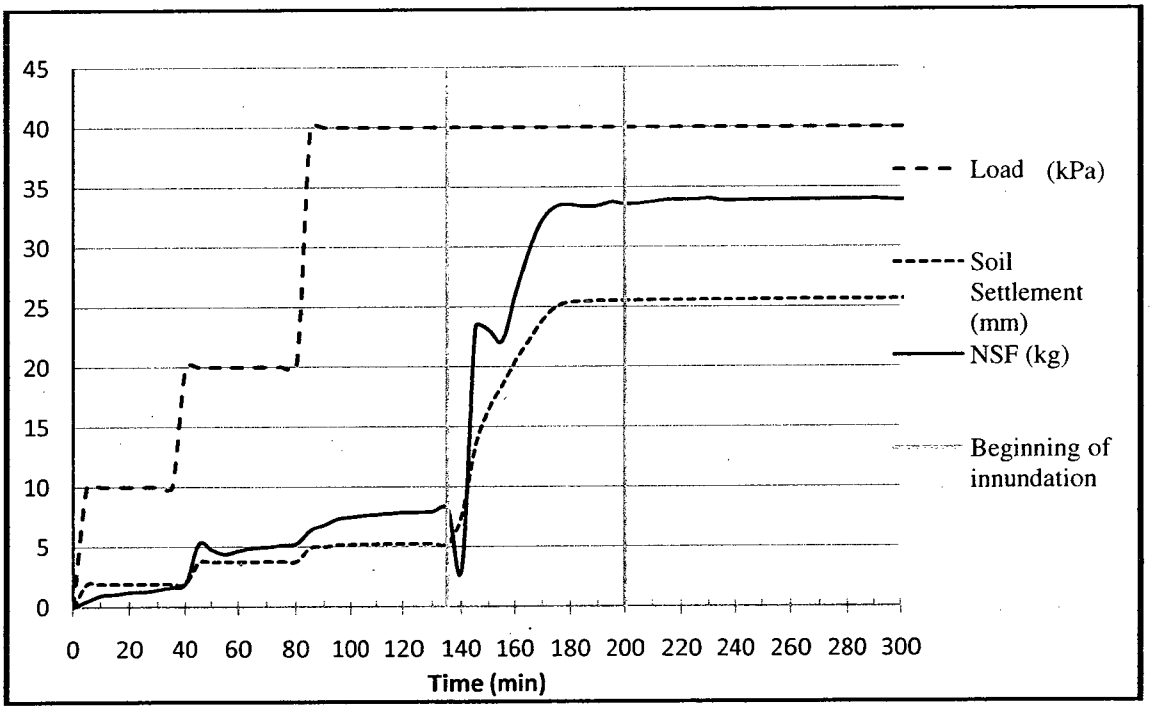

Fig.4.1 Surcharge, settlement and NSF versus time for C_P equal to 12.5% for test number 1

Test Number 2:

In this test, soil mixture 1 with a high collapse potential C_P equal to 12.5% was used, and the soil was inundated at pressure of 60 kPa, results are shown in the figure below

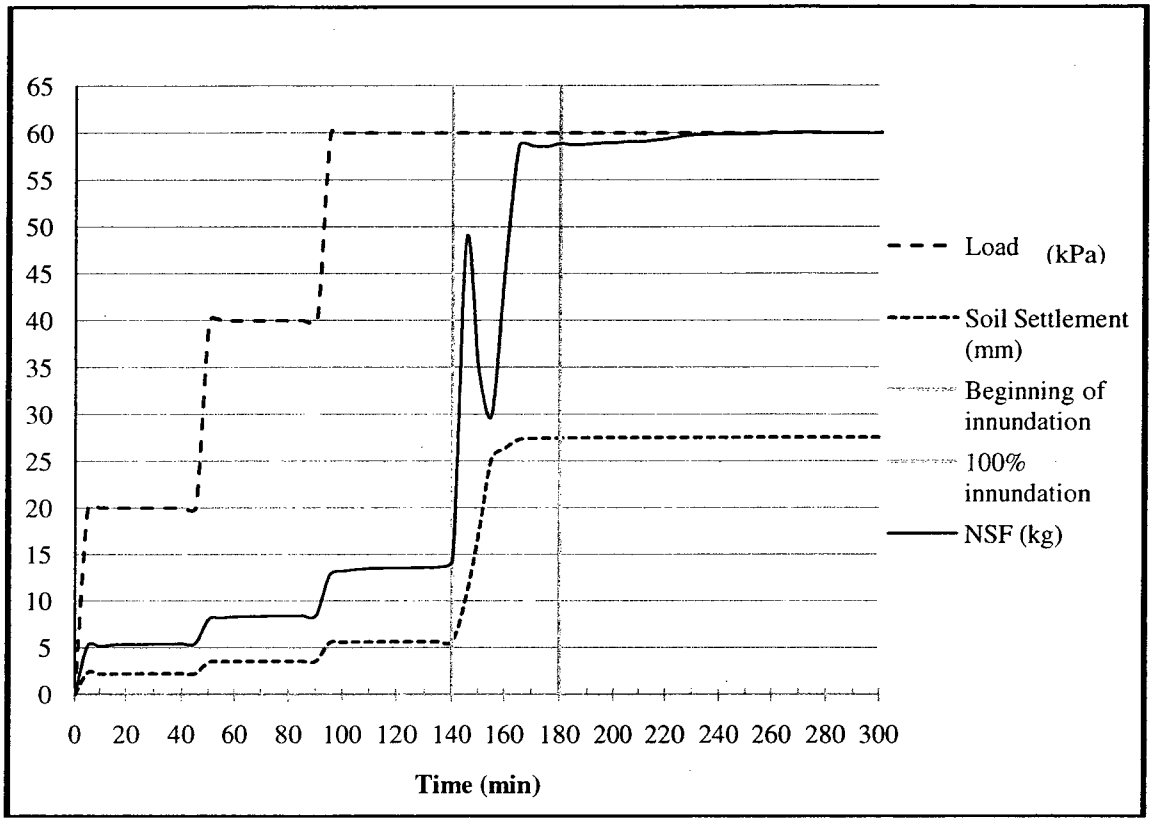

Fig.4.2 Surcharge, settlement and NSF versus time for C_P equal to 12.5% for test number 2

Test Number 3:

In this test, soil mixture 1 with a high collapse potential C_P equal to 12.5% was used, and the soil was inundated at pressure of 80 kPa, results are shown in the figure below

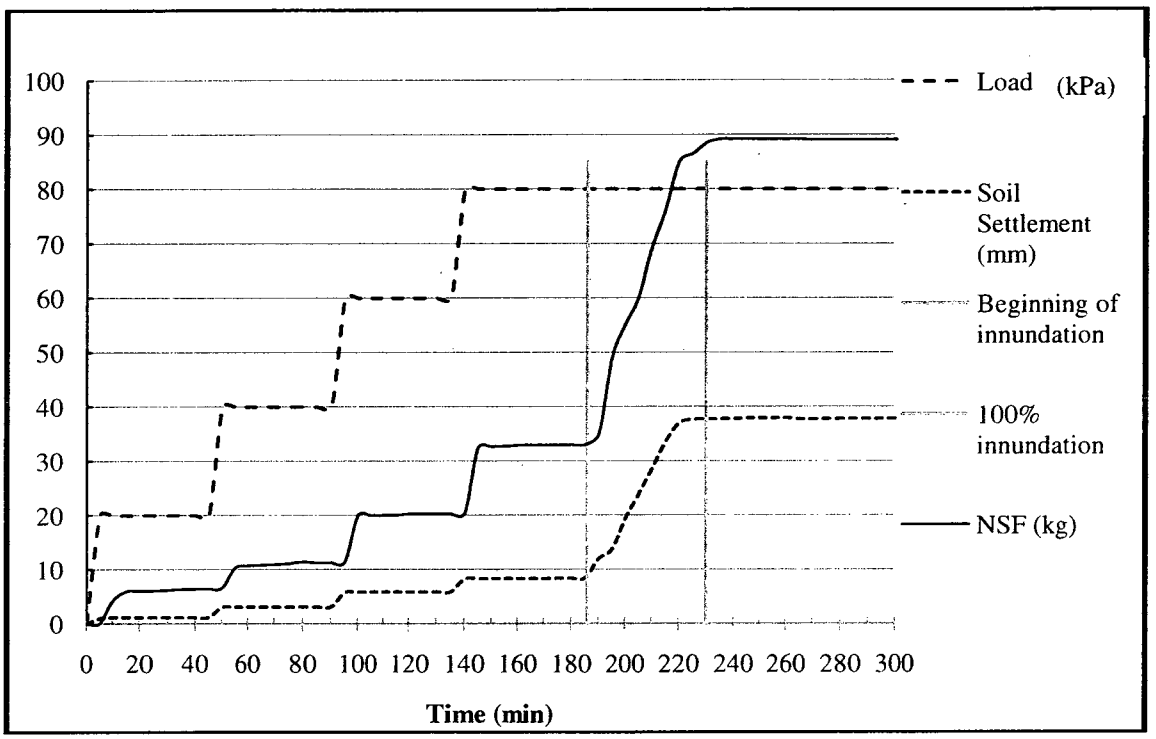

Fig.4.3 Surcharge, settlement and NSF versus time for C_P equal to 12.5% for test number 3

Test Number 4:

In this test, soil mixture 2 with a medium collapse potential C_P equal to 9% was used, and the soil was inundated at pressure of 80 kPa, results are shown in the figure below

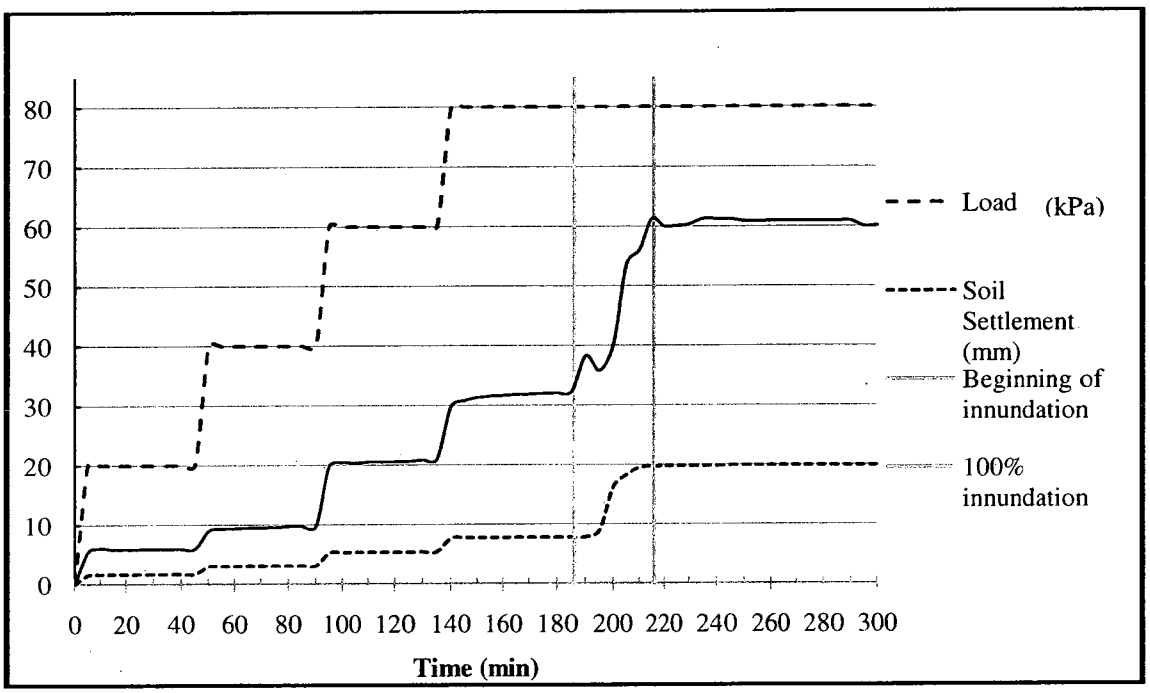

Fig.4.4 Surcharge, settlement and NSF versus time for C_P equal to 9% for test number 4

Test Number 5:

In this test, soil mixture 3 with a low collapse potential C_P equal to 4.2% was used, and the soil was inundated at pressure of 80 kPa, results are shown in the figure below

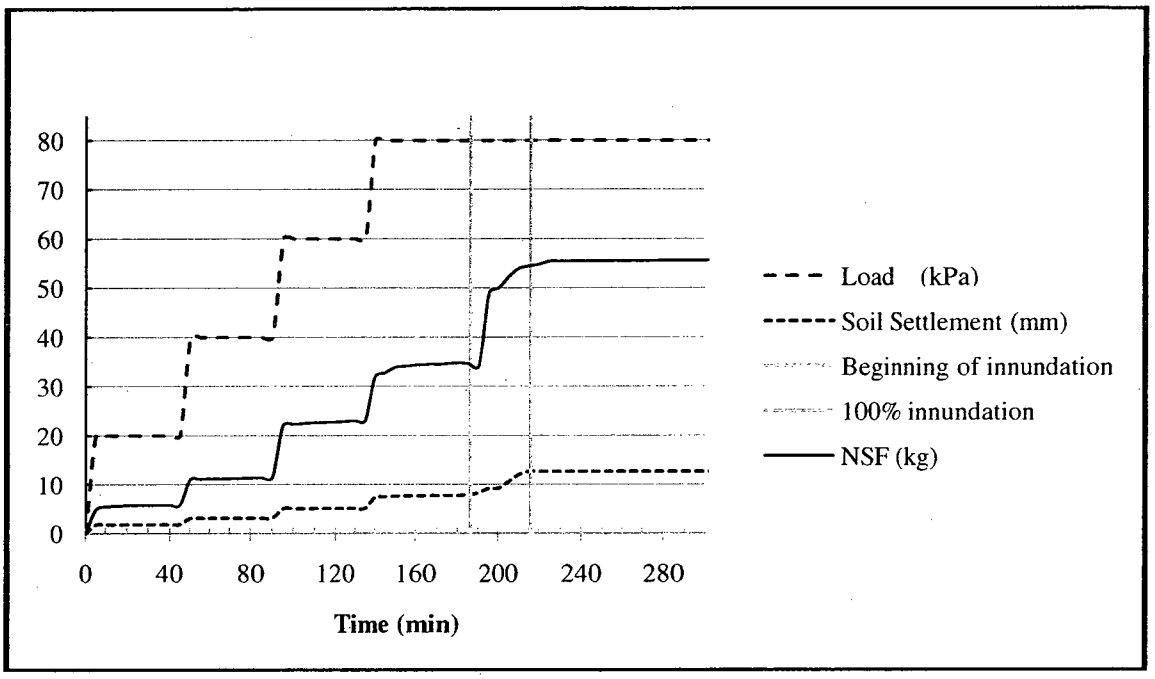

Fig.4.5 Surcharge, settlement and NSF versus time for C_P equal to 4.2% for test number 5

4.4. Parametric Study

In this section the effect of the different governing parameters on negative skin friction was examined.

Figures 4.6 and 4.7 illustrate the relationship between soil strain and time upon soil inundation as obtained from tests. Where fig.4.6 shows the relationship between the soil strain and time for a constant inundation pressure of 80kPa for different collapse potential values, while fig.4.7 shows the relationship between the soil strain and time for a constant collapse potential value C_p=12.5% and for different inundation pressure values.

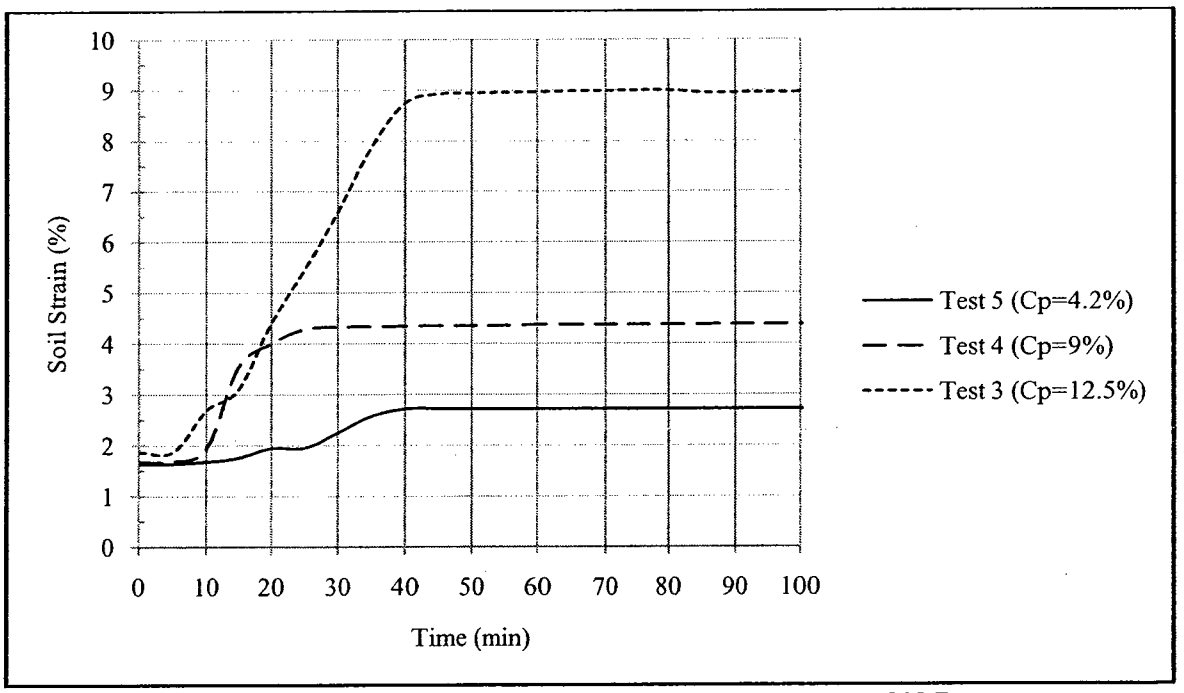

Fig.4.6 The effect of C_p on soil settlement at inundation pressure=80kPa

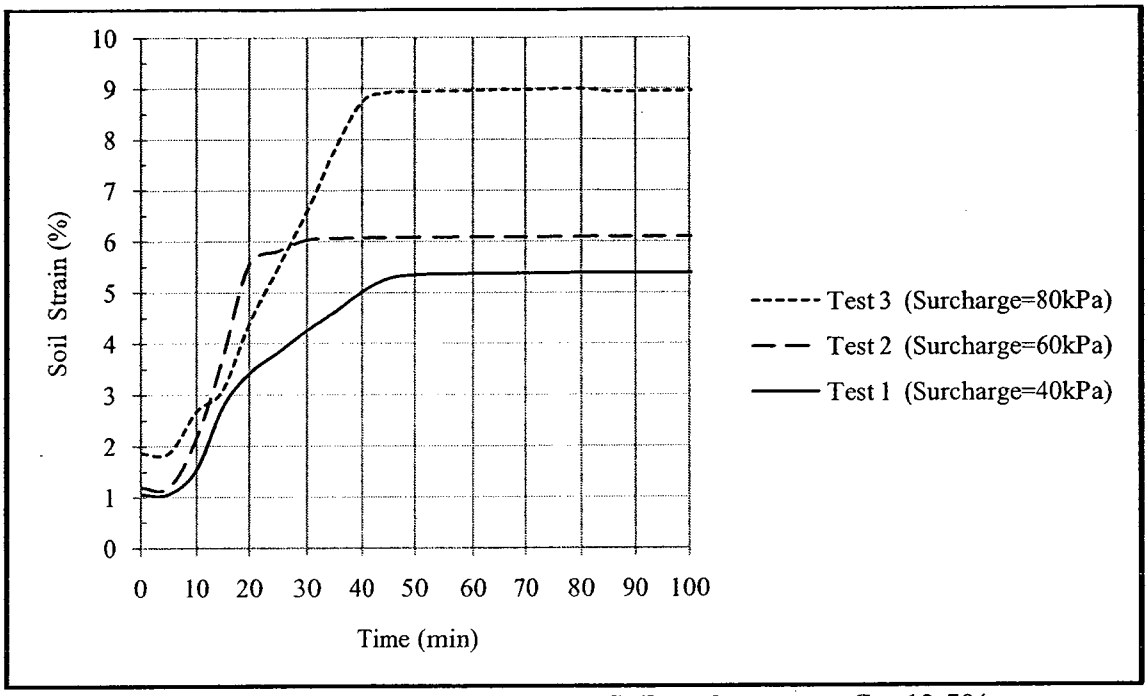

Fig.4.7 The effect of inundation pressure on Soil settlement at C_P =12.5%

Figures 4.8 and 4.9 illustrate the relationship between negative skin friction and time upon soil inundation as obtained from tests. Where fig.4.8 shows the relationship between negative skin friction and time for a constant inundation pressure of 80kPa for different collapse potential values, and fig.4.9 shows the relationship between the negative skin friction and time for a constant collapse potential value C_P =12.5% and for different inundation pressure values.

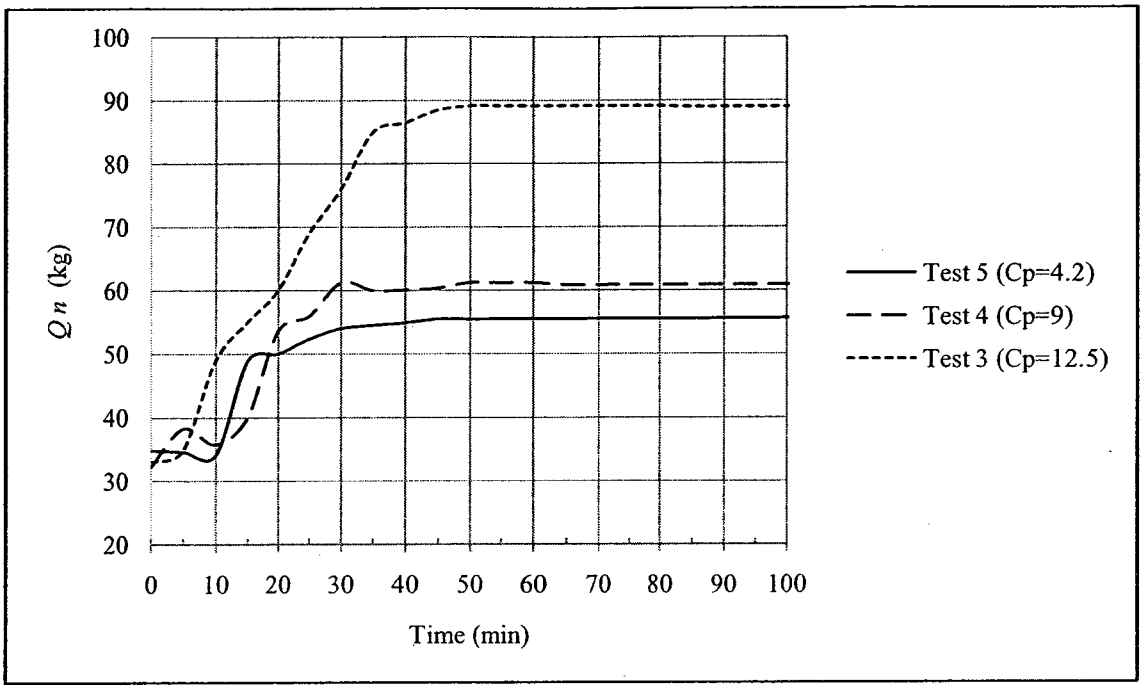

Fig.4.8 The effect of C_P on Negative Skin Friction at inundation pressure=80kPa

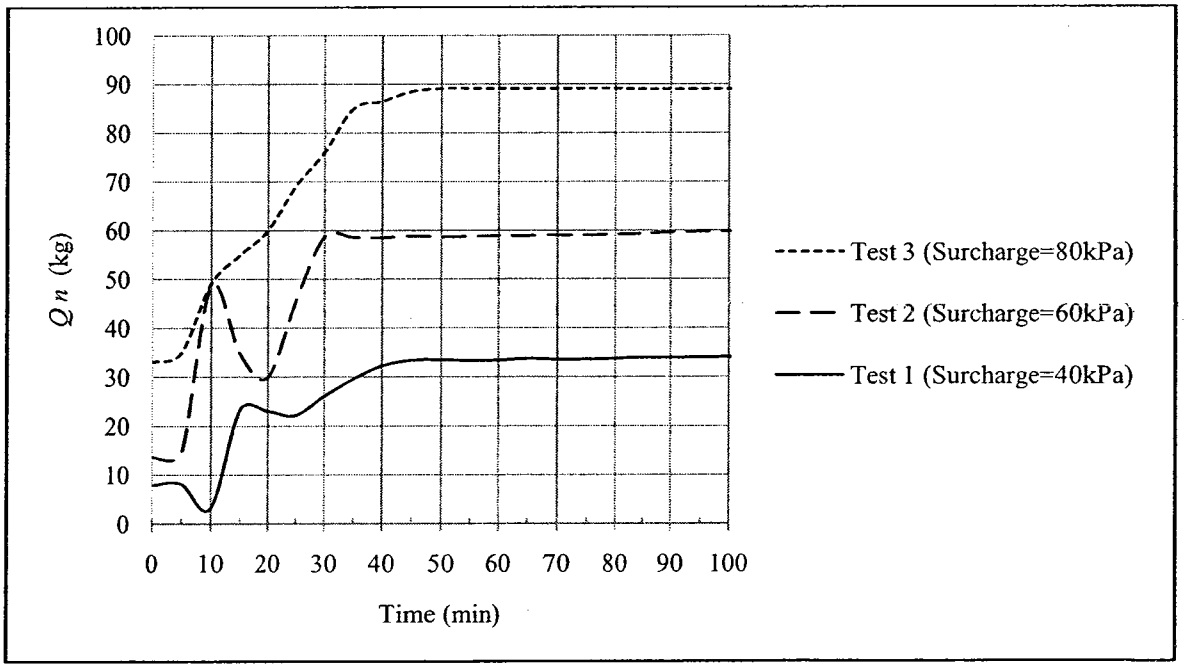

Fig.4.9 The effect of inundation pressure on Negative Skin Friction at C_P =12.5%

For the same inundation pressure; the settlement of soils with different C_P values vary, and accordingly the negative skin friction varies. Also for the same soil with a constant C_P value the settlement under different inundation pressures varies; since the problem of collapsible soils is a problem of large settlement and a radical rearrangement of particles, the soil strain is the most significant value that can define the behavior of the collapsible soil under different circumstances, therefore a relationship between negative skin friction and soil strain was obtained in fig. 4.10 where fig.4.11 shows the relationship between negative skin friction and soil strain for a constant inundation pressure of 80kPa for different collapse potential values, while fig.4.10 shows the relationship between the negative skin friction and soil strain for a constant collapse potential value C_p =12.5% and for different inundation pressure values.

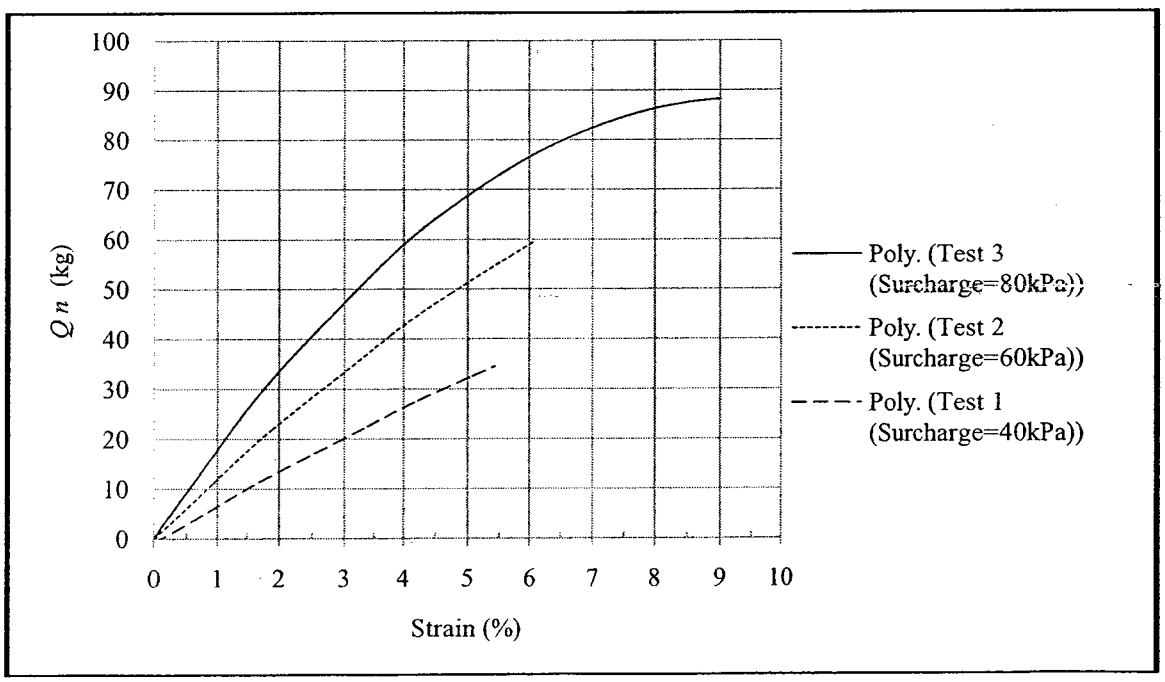

Fig.4.10 The effect of inundation pressure on Negative Skin Friction at C_P =12.5%

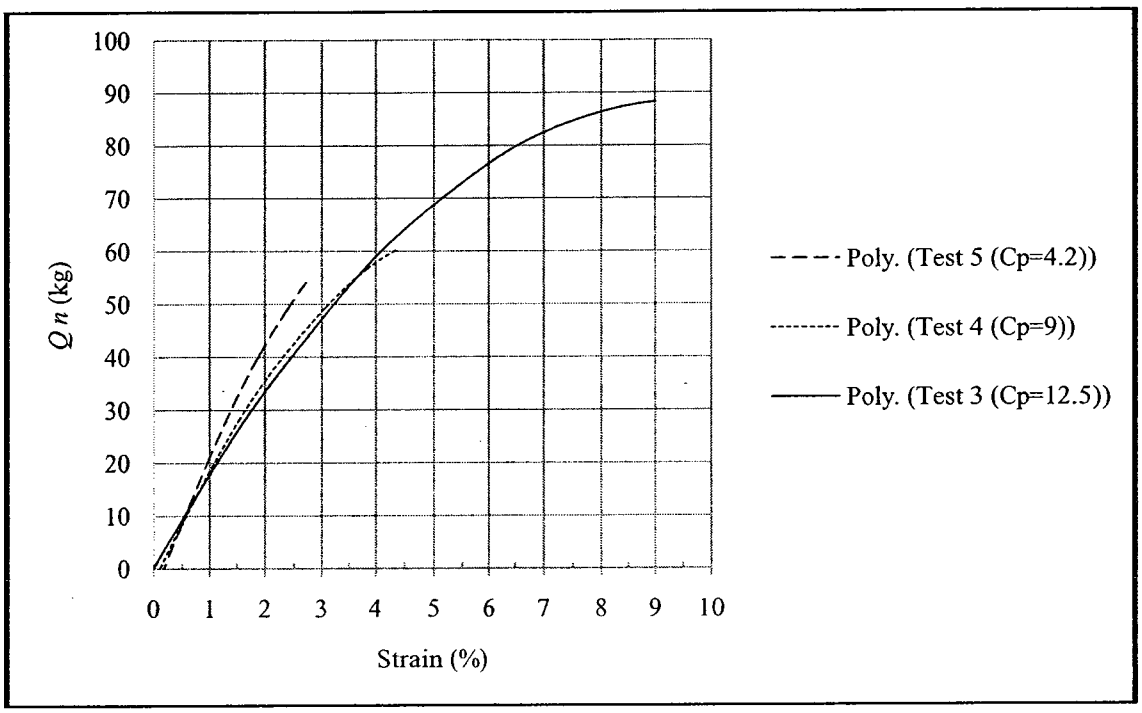

Fig.4.11 The effect of C_P on Negative Skin Friction at inundation pressure=80kPa

There was a sudden, slight drop in negative skin friction upon inundation observed in this study as shown in figures 4.1 and 4.2. This drop in NSF might be explained as a result of stress release due to the introduction of water from downwards to upwards (upward seepage flow), therefore it was only observed only in the first two tests where the surcharge values were 40 and 60 kPa respectively, while for the other tests where a higher surcharge of 80 kPa was applied, there was no drop in NSF, and the effect of the upward seepage flow wasn't observed.

It might also be explained as a result of the particles rearrangement upon wetting, where this drop in NSF takes place under a small surcharge and it takes place, instantly upon introducing water to soil and just before the NSF increases rapidly.

4.5. Analytical Model

After the tests have been performed and results were obtained and presented in figures, analysis of results was aimed at developing a method that could be used by practicing engineers to predict negative skin friction force for piles in collapsible soils based on the tests results obtained in this study.

It was observed from the test results that the negative skin friction increases as the soil settlement and the surcharge increase, and accordingly the negative skin friction increases as the C_p and the inundation pressure increase. This agrees with what was expected based on the literature study.

An extensive effort has been done by many researchers to find accurate values of the negative skin friction coefficient β considering different factors like soil type, bitumen coating, depth of neutral plane and more as discussed in the literature review section.

This study proposes a factor that considers the impact of the collapse behavior of collapsible soil on the negative skin friction force, extending the effective stress method (beta method) for calculating negative skin friction to collapsible soils.

In order to introduce a design procedure and a negative skin friction coefficient $\bar{\beta}$ that takes into consideration the effect of soil collapse upon inundation based on the experimental investigations, an analytical model was established and introduced in this chapter, and accordingly a design procedure for piles in collapsible soils was suggested.

4.5.1 Negative Skin Friction for Piles in Collapsible Soil at Time t After Inundation $Q'_{n(t)}$

As shown in figures 4.8 and 4.9, negative skin friction increases with time upon inundation, until soil is 100% saturated and the collapsible soil settlement is fully mobilized.

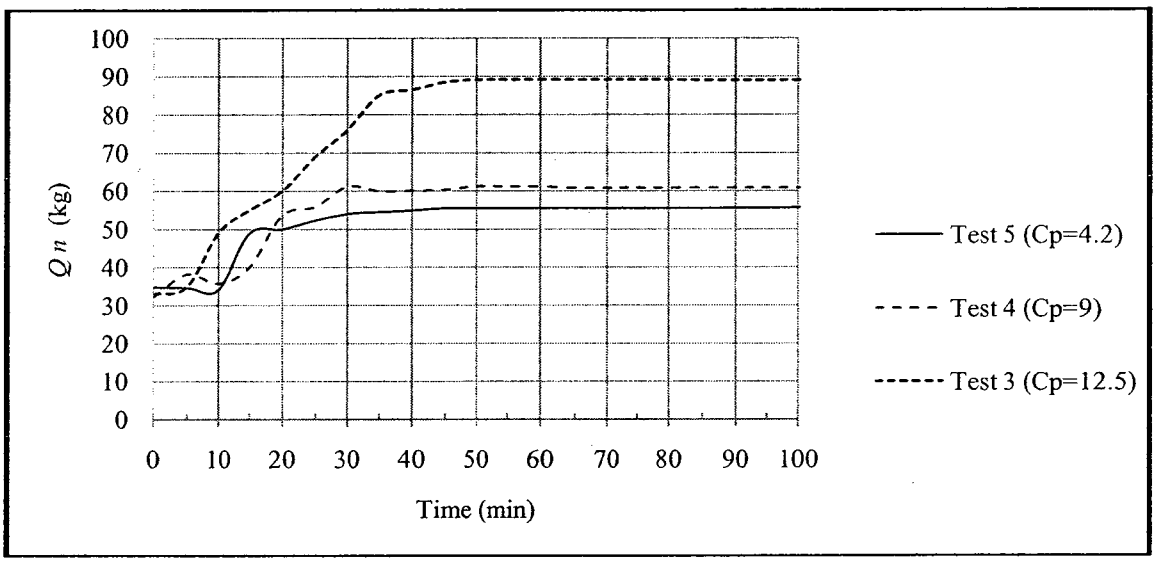

Fig.4.8 The effect of C_P on Negative Skin Friction at inundation pressure=80kPa

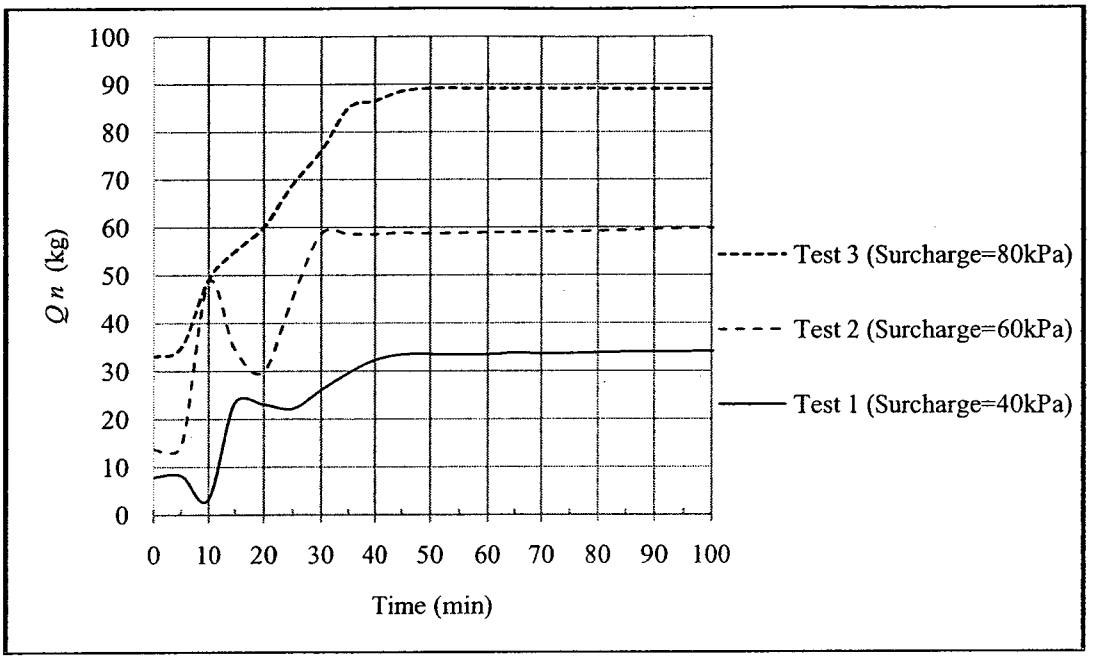

Fig.4.9 The effect of inundation pressure on Negative Skin Friction at C_P =12.5%

The increase in negative skin friction Q'_n with time presented in figures 4.8 and 4.9 is nonlinear; therefore in order to obtain a linear relationship, figures 4.8 and 4.9 were idealized by establishing the relationship between time/Q'_n and time as shown in figures 4.12 and 4.13.

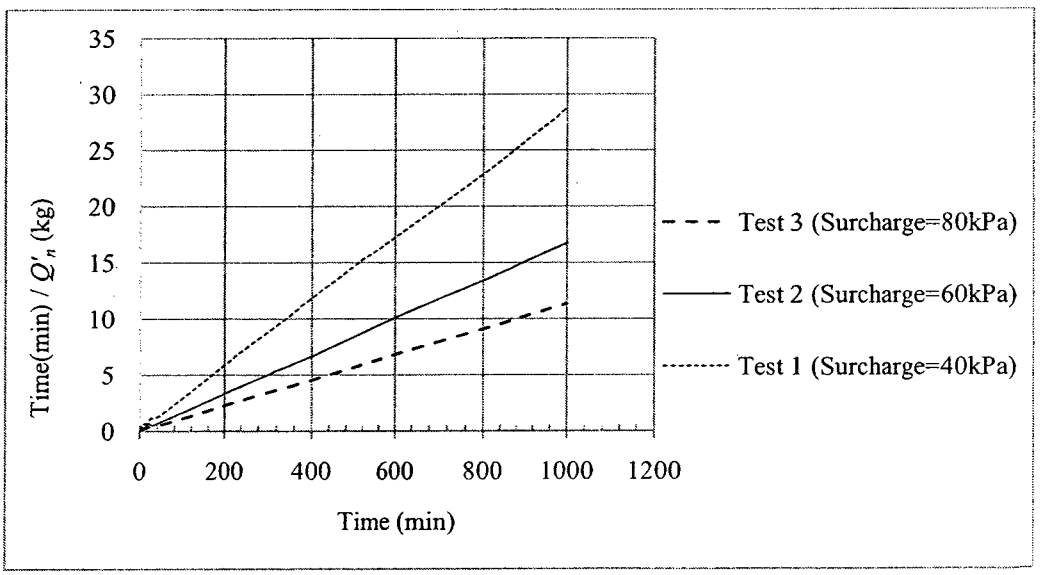

Fig.4.12 The relationship between the time and the time/NSF at C_P =12.5% for inundation pressure values = (40, 60 and 80) kPa

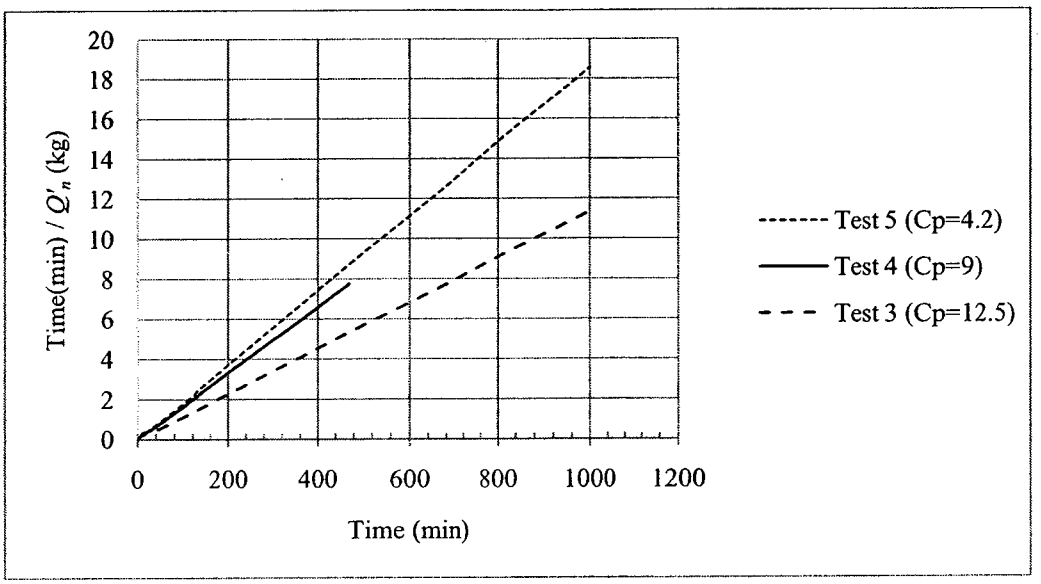

Fig.4.13 The relationship between the time and the time/NSF at inundation pressure=80kPa for C_P values = (12.5, 9 and 4.2) %

The relationship between time/Q'_n and time is a linear relationship as shown in figures 4.12 and 4.13. This relationship was used for establishing equation [4.1] for computing the negative skin friction force at any time t after inundation $Q'_{n(t)}$.

$$Q'_{n(t)} = \frac{t}{at + b} \quad \text{[4.1]}$$

The constants a and b in equation [4.1] were be deduced from the relationship in figures 4.12 and 4.13, where they are both function of the inundation pressure S and collapse potential C_p, therefore the variation of the constants a and b with the inundation pressure S and collapse potential C_p was presented in figures 4.14 and 4.15.

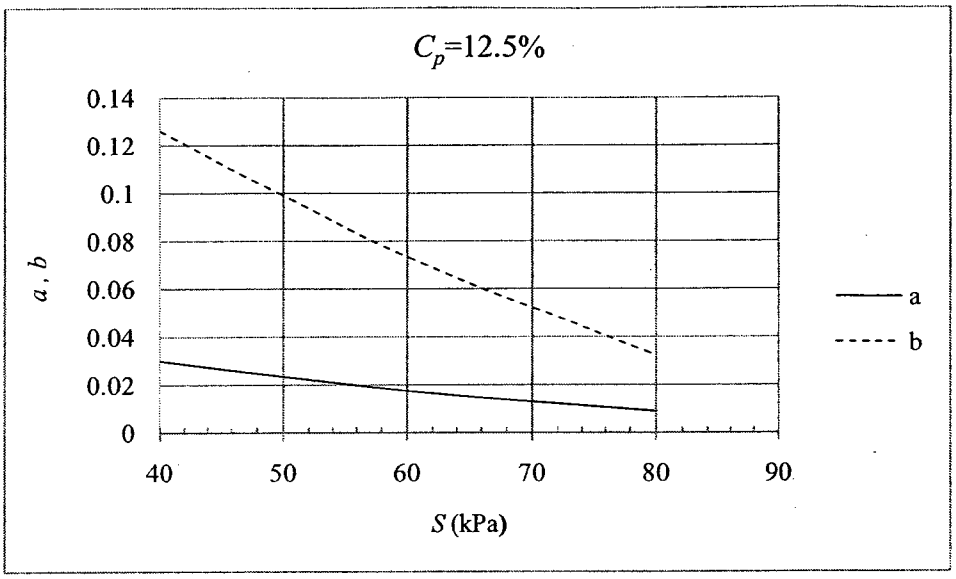

Fig. 4.14 Relationship between *a* and *b* versus inundation pressure *S* (kPa)

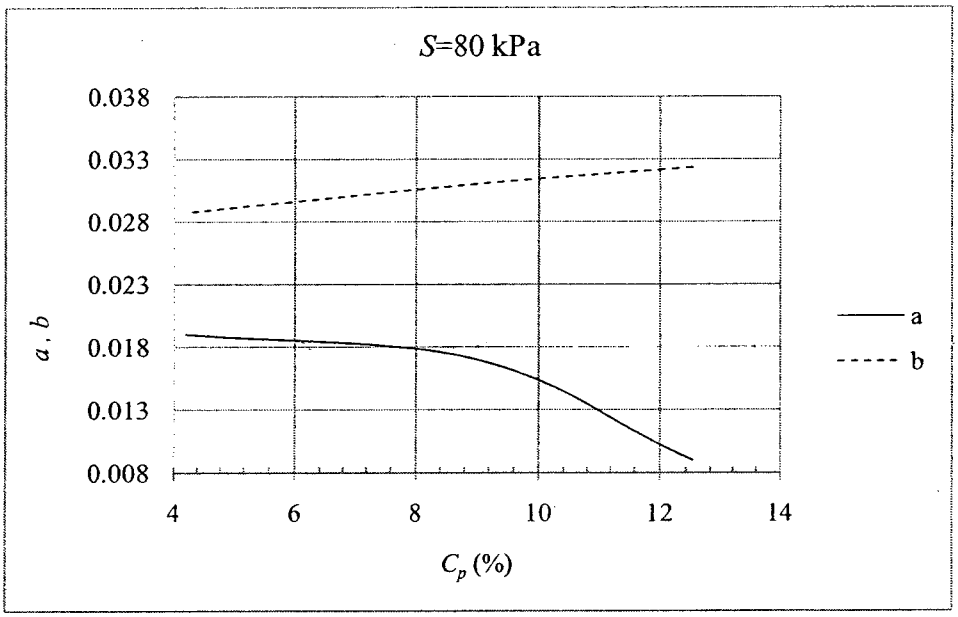

Fig. 4.15 Relationship between *a* and *b* versus collapse potential C_p (%)

From figures 4.14 and 4.15 it can be deduced that b varies linearly with the inundation pressure S as well as collapse potential C_p, therefore the value of the parameter b can be obtained directly from equation [4.3].

Likewise a varies linearly with the inundation pressure S, as well as C_p, where the variation of a with respect to C_p is linear from C_p = 4.2 to 9% and the slope of the line changes for C_p =9 to 12.5%, therefore the value of the parameter a can be obtained directly from equation [4.2].

$$a = k_1 C_P + k_2 S + k_3 \ldots\ldots\ldots\ldots\ldots\ldots\ldots\ldots \quad [4.2]$$

$$b = k_4 C_P + k_5 S + k_6 \ldots\ldots\ldots\ldots\ldots\ldots\ldots\ldots \quad [4.3]$$

Where the values of the constants k_1 through k_6 were deduced from the relationships between a and b versus Cp and S and as shown in figures 4.14 and 4.15 and these values are summarized in table 4.2.

Table 4.2 Constants k_1 through k_6

k_1	For C_p= 0-10	$-1.5*10^{-4}$
	For C_p > 10	$-9.2*10^{-4}$
k_2	-0.00025	
k_3	0.0245	
k_4	0.00025	
k_5	-0.001225	
k_6	0.07825	

4.5.2 Negative Skin Friction Coefficient for Piles in Collapsible Soil $\bar{\beta}$

The maximum negative skin friction for piles in clays $Q_{n(max)}$ can be calculated using equation [9] after (Hanna and Sharif, 2006), where the negative skin friction coefficient β is used.

From the experimental results presented in this study, it was observed that the values of negative skin friction forces accompanied by the inundation of collapsible soil are of a higher magnitude than the forces predicted by equation [2.9], as the equation was proposed for clay and soft soils and it doesn't take into account the effect of the sudden collapse upon inundation in collapsible soils.

There are many factors that contribute to the increase of negative skin friction force upon inundation for collapsible soil, such as the time over which the inundation takes place (inundation rate), the drop in the shear resistance of the soil and the large magnitude of settlement.

The negative skin friction coefficient β changes significantly upon wetting, as the particles experience a significant loss in shear strength, a decreases stress ration and a radical particles rearrangement affecting the value of coefficient of earth pressure K_s and the value of the angle of internal friction φ'.

Therefore a negative skin friction coefficient $\bar{\beta}$ that takes into consideration the effect of soil collapse upon inundation is introduced based on the experimental investigations carried out in this study.

Consequently, in equation [4.4] for calculating the maximum negative skin friction for piles in collapsible soils $Q'_{n(max)}$ the coefficient of negative skin friction for piles in collapsible soils $\bar{\beta}$ was used.

$$Q'_{n(max)} = \int_0^L \bar{\beta}(\pi D)(\gamma' Z + S)\, dz \ldots\ldots\ldots\ldots\ldots\ldots\ldots\ldots\ldots\ldots [4.4]$$

Where:

$Q_{n(max)}$: Maximum negative skin friction force for piles in clays (kPa)

K_s: coefficient of earth pressure

δ': angle of friction between soil and pile shaft, taken: (0.5 to 0.7) φ'

Z: Height of fill (m)

S: surcharge pressure (kPa)

D: Diameter of pile (m)

L: length of pile penetrating settling soil (m)

Equation [4.5] can be used in for obtaining the values of the negative skin friction coefficient for piles in collapsible soil $\bar{\beta}$, where equation [4.5] was deduced from equation [4.4].

$$\bar{\beta} = \frac{Q'_{n(max)}}{\int_0^L (\pi D)(\gamma' Z + S)\, dz} \ldots\ldots\ldots\ldots\ldots\ldots\ldots\ldots [4.5]$$

In order to obtain values of the negative skin friction coefficient for piles in collapsible soil $\bar{\beta}$ from equation [4.5] the value of the maximum negative skin friction $Q'_{n(max)}$ has to be determined.

The maximum negative skin friction values $Q'_{n(max)}$ for the experiments carried out in the current study can be determined using Chin's method after (Chin 1970), where he

proposes that the value of the ultimate load can be obtained by plotting the relationship between time/Q'_n and time as shown in figures 4.12 and 4.13 where the maximum load $Q'_{n(max)}$ is the inverse of the slope of the straight line a in the relationship between time/Q'_n and time, therefore $Q'_{n(max)}$ can be obtained by substituting in equation [4.6].

$$Q'_{n(max)} = \frac{\Delta\left(\frac{t}{Q'_n}\right)}{\Delta t} = \frac{1}{a} \ldots\ldots\ldots\ldots\ldots\ldots\ldots\ldots\ldots \quad [4.6]$$

After obtaining the values of $Q'_{n(max)}$ and by applying in equation [4.6] for the conditions of the experimental tests performed, the values of negative skin friction coefficient for piles in collapsible soil $\bar{\beta}$ were determined and summarized in table 4.3.

Table 4.3 Negative skin friction coefficient $\bar{\beta}$ for the experimental tests

Soil Type	C_p (%)	S (kPa)	φ'	γ (kN/m^3)	L (m)	D (m)	Ks	δ'	β	$Q'_{n(max)}$ (kg)	$\bar{\beta}$
Mix 1	12.5	40.00	35.00	16.20	0.48	0.03	0.43	17.50	0.134	34	0.20
Mix 1	12.5	60.00	35.00	16.20	0.48	0.03	0.43	17.50	0.134	60	0.24
Mix 1	12.5	80.00	35.00	16.20	0.48	0.03	0.43	17.50	0.134	89	0.27
Mix 2	9	80.00	38.50	16.25	0.48	0.03	0.38	19.25	0.132	62	0.19
Mix 3	4.2	80.00	40.00	16.28	0.48	0.03	0.36	17.00	0.130	56	0.17

After obtaining the values of the negative skin friction coefficient $\bar{\beta}$ for the experimental tests, the variation of β and $\bar{\beta}$ with respect to S and C_p was plotted in figures 4.16 and 4.17.

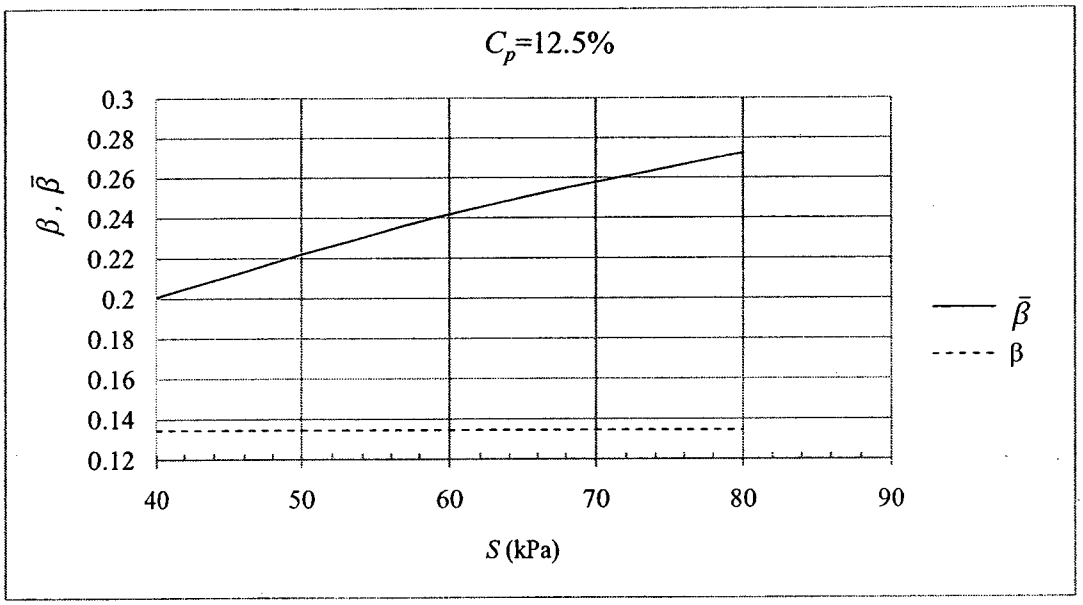

Fig. 4.16 Relationship between β, $\bar{\beta}$ and S for C_p=12.5%

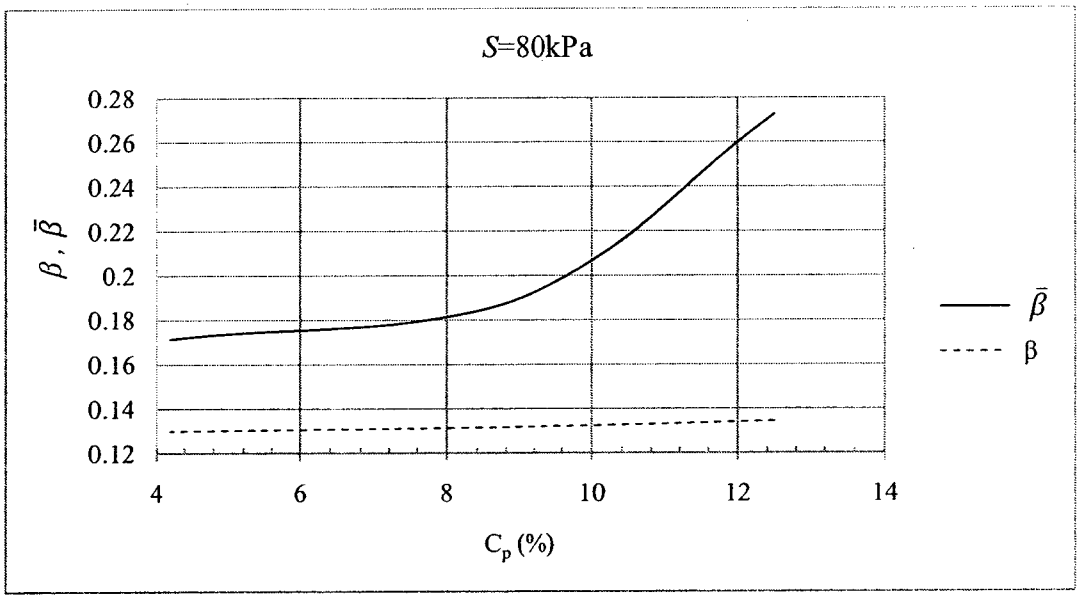

Fig. 4.17 Relationship between β, $\bar{\beta}$ and C_p for S=80 kPa

From figures 4.17 and 4.18 it can deduced that β and $\bar{\beta}$ vary linearly with the inundation pressure S, as well as C_p, where the variation of $\bar{\beta}$ with respect to C_p is linear from C_p = 4.2 to 9% and the slope of the line changes for C_p =9 to 12.5%, therefore the value of the $\bar{\beta}$ can be obtained directly from equation [4.7].

$$\bar{\beta} = k_7 C_P + k_8 S + k_9 \ldots\ldots\ldots\ldots\ldots\ldots\ldots\ldots\ldots \quad [4.7]$$

The values of k_7, k_8 and k_9 were deduced from the relationships between $\bar{\beta}$ versus C_p and $\bar{\beta}$ versus S, as shown in figures 4.16 and 4.17 and summarized in table 4.4.

Table 4.4 Constants k_7, k_6 and k_9

K_7	For C_p= 0-10	$1.6*10^{-3}$
	For C_p > 10	$1.5*10^{-4}*S$
K_8	$1.075*10^{-3}$	
K_9	0.079	

In order to validate equation [4.7], figure 4.18 was plotted to compare the values of the maximum negative skin friction $Q'_{n(max)}$ as measured from the experiments carried out in the current study, versus the calculated values of maximum negative skin friction $Q'_{n(max)calc.}$ obtained from equation [4.5], where $\bar{\beta}$ in equation [4.5] was obtained from equation [4.7]. From figure 4.18 it is shown that the maximum error resulted in equation [4.7] was of 7 %.

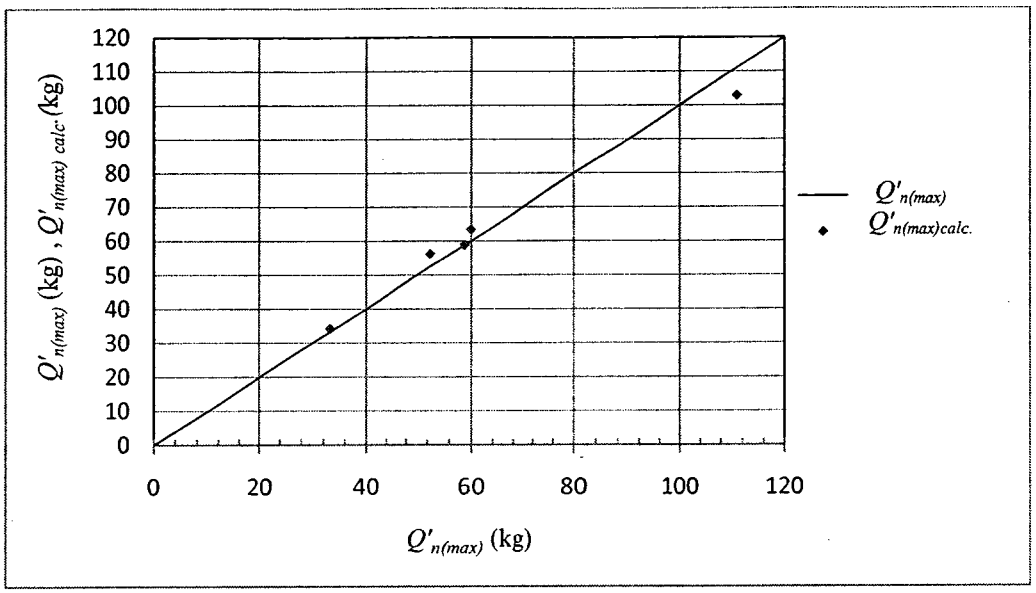

Fig 4.18 The maximum measured negative skin friction $Q'_{n(max)}$ versus the maximum calculated negative skin friction $Q'_{n(max)calc.}$

4.5.3 Correction Factor for Negative Skin Friction on Piles in Collapsible Soil R_c

Since the value of $\bar{\beta}$ is higher than that of β as shown in figures 4.16 and 4.17, a correction factor R_c is proposed for considering the effect of collapsible soil, where R_c is equal to $\bar{\beta}$ over β as show in equation [4.9] and it can be obtained from figures 4.19 and 4.20, and thus $Q'_{n(max)}$ can be calculated from equation [4.8].

$$Q'_{n(max)} = R_C\, Q_{n(max\ )} \ldots\ldots \quad [4.8]$$

Where:

$$R_c = \frac{\bar{\beta}}{\beta} \ldots\ldots\ldots\ldots\ldots\ldots\ldots\ldots\ldots \quad [4.9]$$

From equation [4.9], the relationships between R_c versus collapse potential C_p and R_c versus inundation pressure S were plotted as shown in figures 4.19 and 4.20.

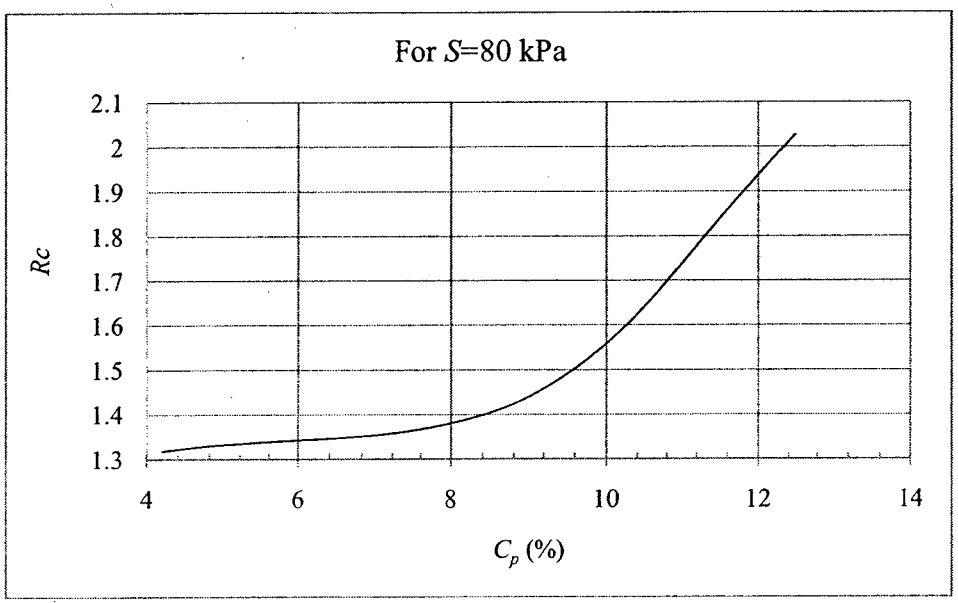

Fig. 4.19 Relationship between R_c and C_p for S=80 kPa

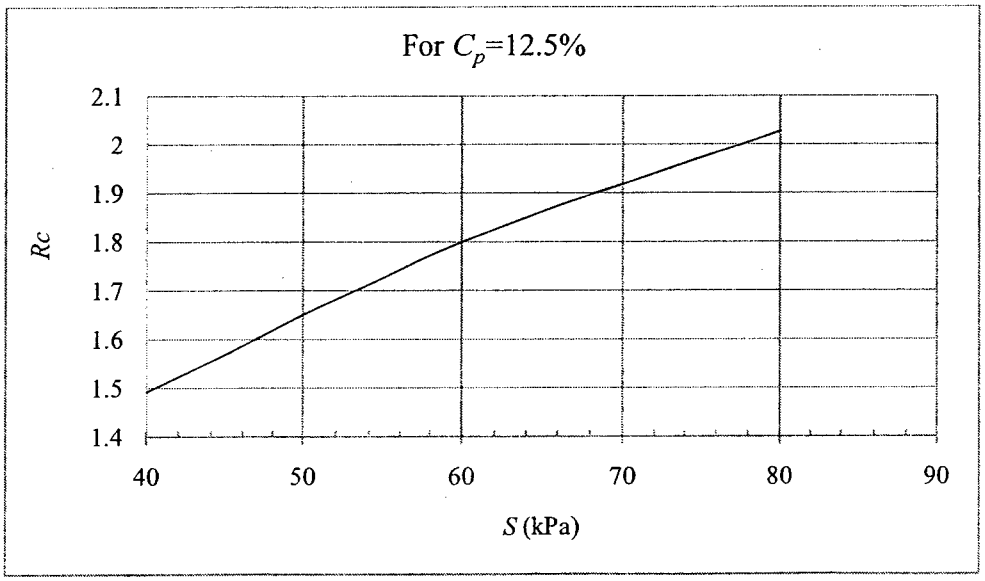

Fig. 4.20 Relationship between R_c and S for C_p=12.5%

From the relationships between R_c versus C_p and R_c versus S, as shown in figures 4.18 and 4.19, equation [4.10] was deduced for obtaining the value of the correction factor Rc as a function in collapse potential Cp, inundation pressure S and angle of internal fiction φ'.

Where:

$$\beta = Ks \tan \delta' \ldots\ldots\ldots\ldots\ldots\ldots\ldots\ldots\ldots\ldots \quad [2.8]$$

$$K_S = 1 - sin\varphi' \ldots\ldots\ldots\ldots\ldots\ldots\ldots\ldots\ldots\ldots \quad [4.11]$$

$$R_c = \frac{\bar{\beta}}{\beta} = \frac{k_7 C_P + k_8 S + k_9}{(1 - sin\varphi') \tan \delta'} \geq 1.0 \ldots\ldots \quad [4.10]$$

The friction angle between the soil and pile δ' was assumed to be 0.5 φ' as the pile used in the experiments was a steel pile of a rough surface, while the coefficient of earth pressure K_S in equation [2.8] was assumed to be at rest ie. K_o, therefore K_S can be calculated using equation [4.11].

4.5.4 Design Charts

Design charts were suggested in figures 4.21 through 4.25 in order to obtain the correction factor R_c, that takes into account the effect of collapsible soil when calculating negative skin friction forces for single piles. The correction factor R_c is presented in the design charts as a function in the collapse potential C_p, inundation pressure S and angle of internal friction φ'. Where the values presented in the design charts were obtained by substituting in equation [4.10].

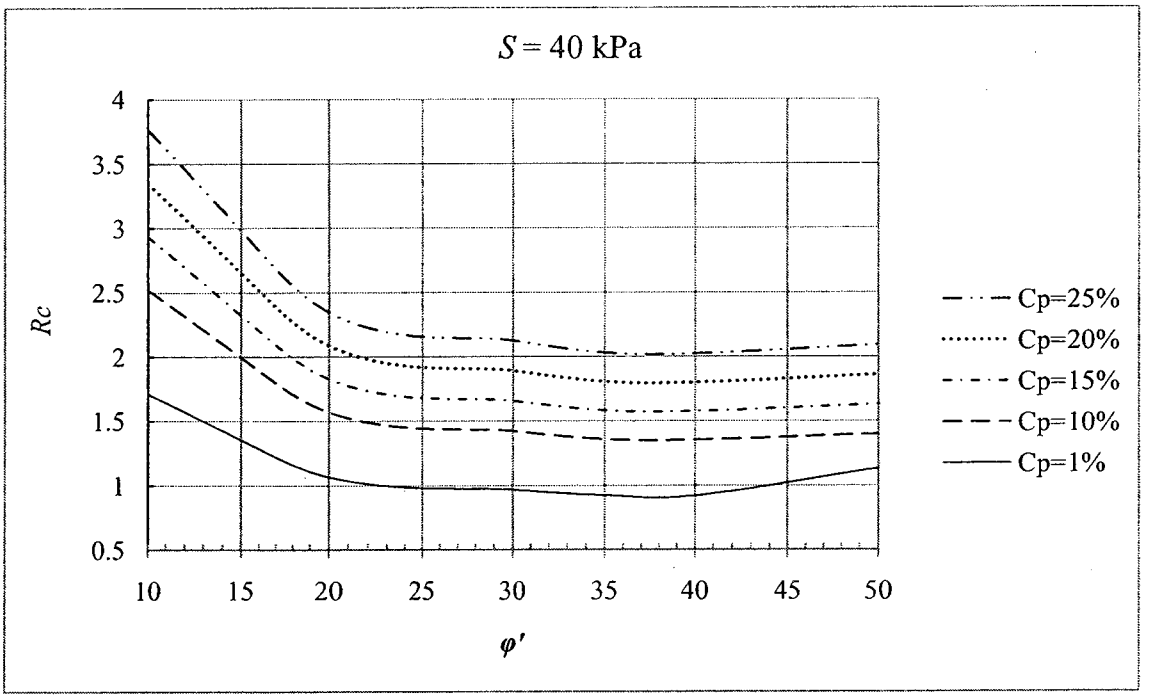

Fig. 4.21 Design chart for obtaining R_c by knowing C_p *and* φ', for S=40 kPa

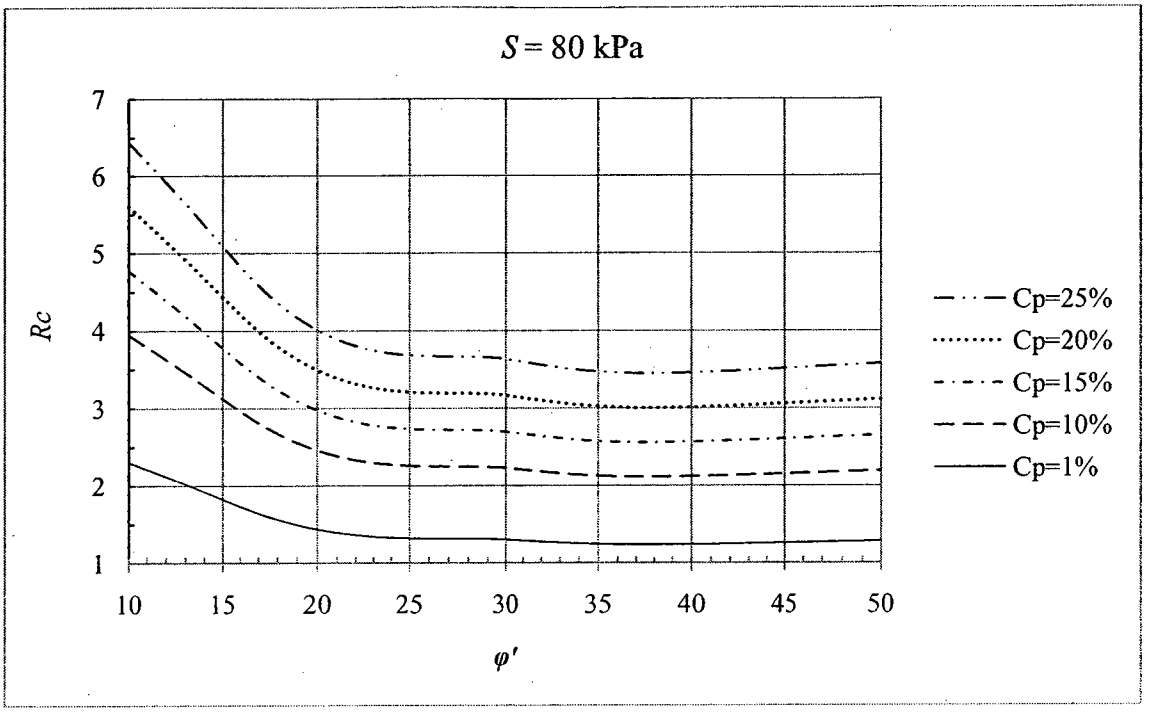

Fig. 4.22 Design chart for obtaining R_c by knowing C_p *and* φ', for S=80 kPa

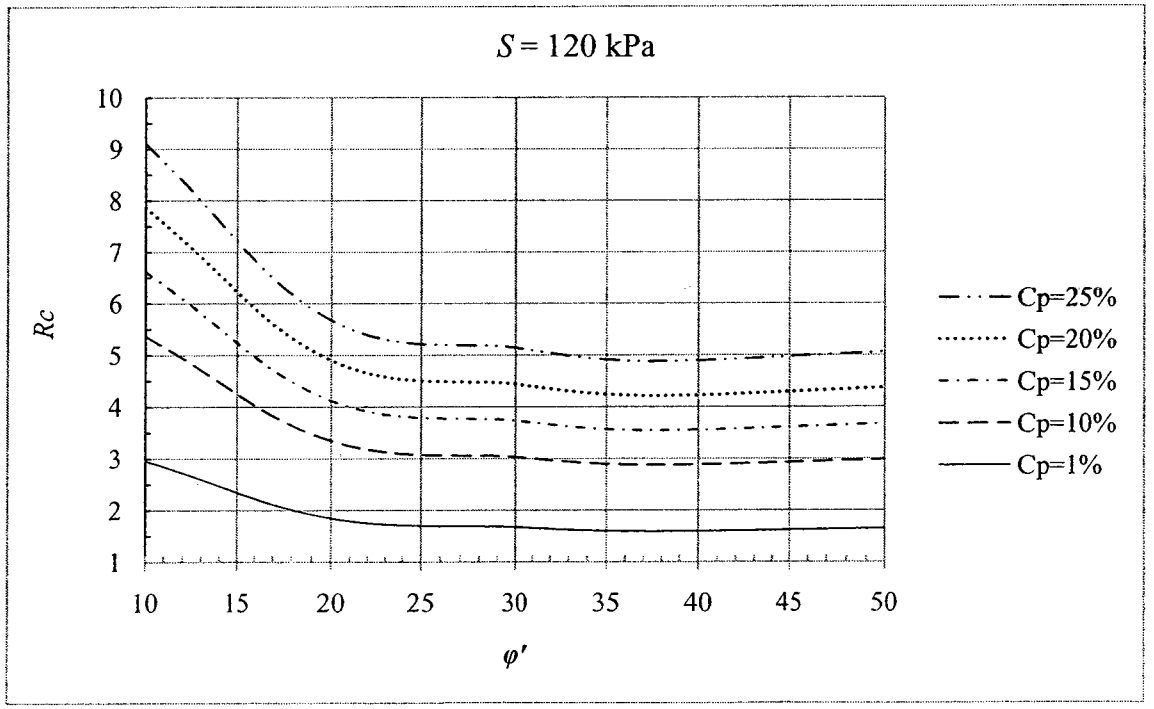

Fig. 4.23 Design chart for obtaining R_c by knowing C_p *and* φ', for S=120 kPa

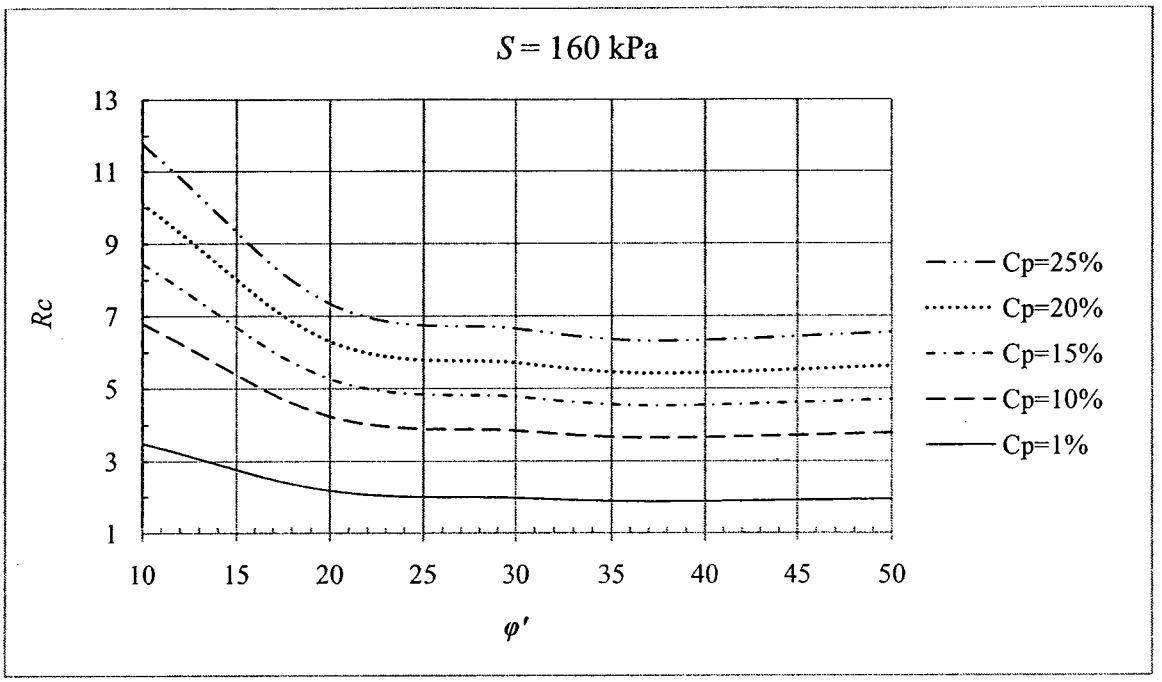

Fig. 4.24 Design chart for obtaining R_c by knowing C_p *and* φ', for S=160 kPa

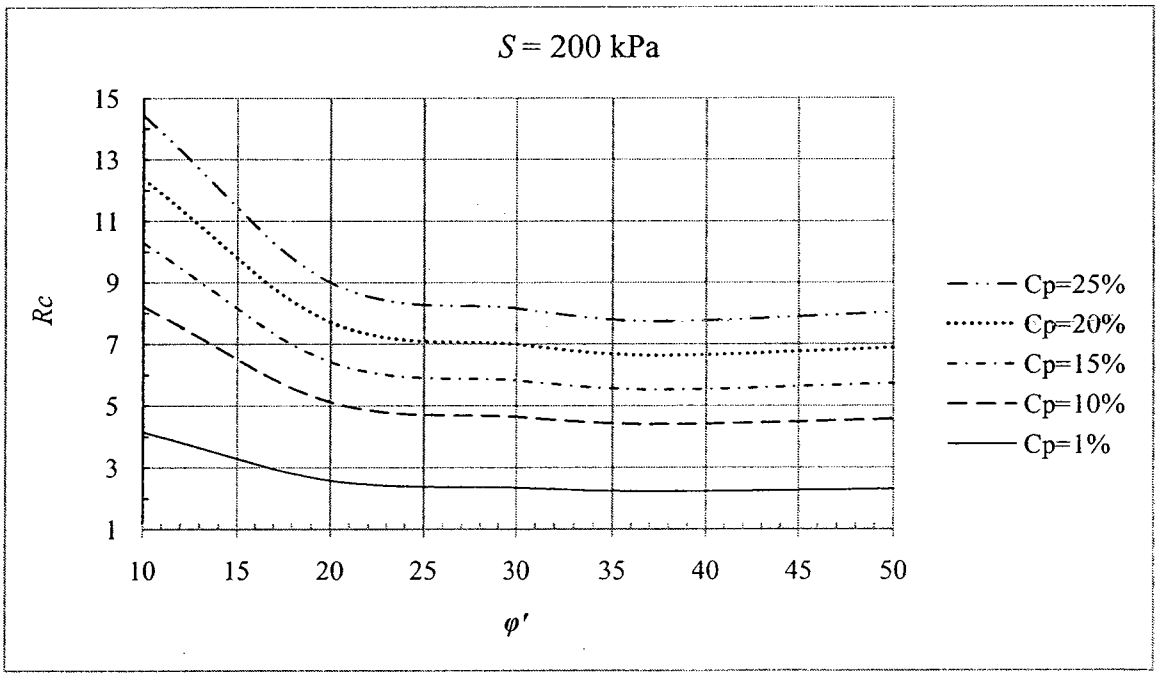

Fig. 4.25 Design chart for obtaining R_c by knowing C_p *and* φ', for S=200 kPa

4.6 Design Procedure for Negative Skin Friction for Piles in Collapsible Soils

After introducing equations obtained by the analytical model for computing negative skin friction on piles in collapsible soils, a design procedure is proposed in this section.

Step 1:

For obtaining the maximum negative skin friction force acting on piles in collapsible soil $Q'_{n(max)}$:

a. Obtain $Q_{n(max)}$ from equation [2.9], knowing the soil properties: (γ, φ', Z)
b. Find the value of R_c From figure 4.12, knowing C_p and S.
c. Calculate $Q'_{n(max)}$ from equation [4.9], knowing R_c and $Q_{n(max)}$.

Step 2:

For obtaining the allowable bearing of the pile Q_a:

The theory proposed by (Hanna and Sharif, 2006) is one of the well established theories that is based on field results and numerical analysis, and it takes into account the effect of neutral plane depth and the bitumen coating. Applying the correction factor R_c to the equation proposed (Hanna and Sharif, 2006) to calculate the allowable load to be applied on the piles, equation [4.12] is proposed for end-bearing piles in collapsible soils.

$$Q_a = \left[\frac{Q_t + Q_s}{FS} - Q'_{n(max)}\right] \ldots\ldots\ldots\ldots\ldots \quad [4.12]$$

Step 3:

If the designer is interested in computing the negative skin friction force at any time t after inundation $Q'_{n(t)}$ equation [4.1] can be used.

CHAPTER 5

CONCLUSIONS AND RECOMMENDATIONS

5.1. General

Based on the results obtained from the experimental investigation and the analysis presented in the current study, conclusions were drawn and presented in this chapter and recommendations for further research were provided.

5.2. Conclusions

An experimental investigation was conducted to examine the negative skin friction forces acting on single piles in collapsible soils due to soil inundation.

Based on the results obtained from the present experimental investigation, and the analytical model the following conclusions can be drawn:

1. The collapsible soil induces negative skin friction forces of a higher magnitude than that computed by conventional methods used for clays and other types of soft soils.
2. The parameters governing the settlement of the collapsible soils are collapse potential C_p, inundation pressure S, the rate of inundation, thickness and shear strength of the collapsible layer.
3. Negative skin friction force on single piles in collapsible soil increases due to an increase of collapse potential C_p, inundation pressure S, the rate of inundation, thickness of the collapsible layer and decreases due to an increase of the shear strength of the collapsible soil.

4. Analytical model was developed for predicting the negative skin friction acting on single piles in collapsible soils at time t after inundation $Q'_{n(t)}$ and the maximum negative skin friction force $Q'_{n(max)}$. Design procedure and design charts are presented for the use of practicing engineers.

5.3. Recommendations for further research

1. The current experimental model was a prototype model, yet a full scale model should be used to confirm the results.
2. Pile group effect should be examined for these piles.
3. The effect of layered soil should be studied, especially the case of weaker soil underlying a collapsible soil layer.
4. Effect of bitumen coating, different pile material and pile sections should be studied.
5. Effect of pile installation method (driven and bored piles) should be examined.

REFERENCES

1. **Auvinet, G. and Hanel, J. J. (1981).** " Negative skin friction on piles in Mexico City clay". Proceedings, 10th International Conference on Soil Mechanics and Foundation Engineering, Stockholm, Sweden, pp. 599-604.
2. **Bara, J. P., (1976).** "Collapsible Soils," ASCE Annual Conv. Exposition, Sept., Philadelphia, Pa.
3. **Barden, L., McGown, A. and Collins, K., (1973).** "The collapse Mechanism in Partly Saturated Soil", Engineering Geology, Vol. 7, pp. 49-60.
4. **Beckwith, G. (1995).** "Foundation Design Practices for Collapsing Soils in the Western United States in Unsaturated Soils". In Proceedings of the First International Conference on Unsaturated Soils, E.E. Alonso and P. Delage (eds), Vol. 2, Paris, September. Balkema, Rotterdam.
5. **Begemann, H.K.S., (1969)** "The Dutch static penetration test with the adhesion jacket cone", Lab. Grondmech. Delft, Meded., 12 (4), 69-100; 13 (1), 1-86.
6. **Bjerrum L. Johannessen, I.J., and Eide, O., (1969).** "Reduction of negative skin friction on steel piles to rock". Proceedings 7th International Conference on Soil Mechanics and Foundation Engineering, Mexico City, August 25 - 29, Vol. 2, pp. 27 - 34.
7. **Blessey, W. E., (*1970*).** 'Allowable *Pile Capacity*, Mississippi Deltaic Plain" Proceedings of Design Installation of Pile Foundations, Lehigh University Bethlehem, Pa, pp 87-106.

8. **Bozozuk, M., and Labrecque, A. (1969).** "Downdrag measurement on 270-ft composite piles". In Proceedings of the Symposium on Performance of Deep Foundations, San Francisco, American Society for Testing and Materials (ASTM), Special Technical Publication STP 444, pp. 15–40.
9. **Bozozuk, M., (1972).** "Downdrag measurement on 160-ft floating pipe test pile in marine clay". Canadian Geotechnical Journal, Vol. 9, No. 2, pp. 127-136.
10. **Briaud, J.L., (1997).** "Bitumen Selection for Downdrag on Piles," Journal of Geotechnical and Geoenvironmental Engineering, Vol. 123, No. 12, ASCE, New York, December.
11. **Burland, J. B. (1973),** "Shaft friction piles in clay—A simple fundamental approach", Ground Engineering, 6(3), pp. 30–42.
12. **Burland, J.B. and Starke, W. (1994).** "Review of measured negative pile friction in terms of effective stress". Proc. of 13th International Conference on Soil Mechanics and Foundation Engineering, New Delhi, pp. 493 – 496.
13. **Chin, F.K. (1970).** "Estimation of the Ultimate Load of Piles Not Carried to Failure", Proc.2nd Southeast Asia. Conference on soil Engineering, pp. 81-90.
14. **Chow, Y. K., Chin, J. T., and Lee, S. L. (1990).** "Negative skin friction on pile groups." Int. J. Numer. Analyt. Meth. Geomech., 14, pp. 75–91.
15. **Clemence, S.P., Finbarr, A.O., (1981).** "Design consideration for collapsible soils". Journal of Geotechnical Engineering, ASCE 107 (GT3), pp. 305– 317.
16. **Clemente, F. M., (1981).** "Downdrag on bitumen coated piles in a warm climate". Proceedings of the 10th International Conference on Soil Mechanics and Foundation Engineering, Stockholm, Vol. 2, pp. 673 - 676.

17. **Darragh. R.D., and Bell, R.A. (1969),** "Load Tests on Long Bearing Piles." In Performance of Deep Foundations, Special Techrnical Publication 444, American Society for Testing and Materials, pp. 41-67.

18. **Eide, O., Hutchinson, J. N. & Landva, A., (1961).** "Short and long term test loading of a friction pile in clay". Proc. Fifth Znt. Conf Soil Mech. Fdn Engng, Paris, pp. 45-54.

19. **Endo M., Minou, A., Kawasaki T, and Shibata, T., (1969).** "Negative skin friction acting on steel piles in clay". Proc. 7th International Conference on Soil Mechanics and Foundation Engineering, Mexico City, August 25 - 29, Vol. 2, pp. 85 - 92.

20. **Evstatiev, D., (1995).** "Design and treatment as loess bases in Bulgaria. In:Genesis and properties of collapsible soils", Edited by Ed. Derbyshire (Ed.- in - Chief), T. Dijkastra, J. Smalley, NATO ASI Series C: Matematical and Physical Scienses vol. 468, Kluwer Akad. Publishers, pp. 375 - 382.

21. **Fellenius, B., (1955).** "Results of Tests on Piles at Gothenburg Railway Station". Bulletin No. 5, Geotechnical Department, Swedish State Railways.

22. **Fellenius, B. H. and Broms, B. B., (1969).** "Negative skin friction for long piles driven in clay". Proc. 7th ICSMFE, Mexico City, Vol. 2, pp. 93-98.

23. **Fellenius, B.H., (1972).** "Downdrag on piles in clay due to negative skin friction". Canadian Geotechnical Journal, 9(4), pp. 323–337.

24. **Fellenius, B. H., (1989).** "Unified design of piles and pile groups". Transportation Research Board, Washington, TRB Record 1169, pp. 75 - 82.

25. **Gao, X. J., Wang, J. C., Zhu, X. R., (2007).** "Static load test and load transfer mechanism study of squeezed branch and plate pile in collapsible loess foundation," Journal of Zhejiang University - Science A, 8(7), pp. 1110-1117.

26. **Garlanger, J. E., (1972).** "Prediction of the Downdrag Load at Culter Circle Bridge," Conference, Massachusetts Institute of Technology, Cambridge, Mass.

27. **Garlanger, J. E., (1974).** "Measurement of Pile Downdrag beneath a Bridge Abutment," Highway Research Board, Tra-?S. Res. Record No. 5 17, pp. 6 1-69.

28. **Garneau, R., (1974).** "Capacite de Pieux Flottants dans une Argile Molle," Proceedings Conference of the Quebec Good Roads Association, Quebec, Canada, pp.42-64.

29. **Grigoryan, A.A., and. Grigoryan, R. G (1975).** "Experimental investigation of "negative-friction" forces along the lateral surface of piles as the soils experience slum-type settlement under their own weight," Osn., Fundam. Mekh. Gruntov, No. 5, pp. 10-13.

30. **Grigoryan, A.A., and Yushube, S.V. (1986).** "Interaction between bored-cast-in-place piles and soils under Type II collapsibility conditions," Osn., Fundam. Mekh. Gruntov, No. 2, pp. 14-17.

31. **Grigoryan, A. A. and Chinenkov, Yu. A. (1990).** "Experience gained with construction on long piles with broadened heels in soils prone to slump-type settlement," Osn., Fundam. Mekh. Gruntov, No. 4, pp. 2–5.

32. **Grigoryan, A. A. (1991).** "Construction on loess soils", Osn., Fundam. Mekh. Gruntov, No. 1, pp. 24–27

33. **Grigorian, A., A., (1997).** "Pile foundations for buildings and structures in collapsible soils" Publisher Rotterdam; Brookfield, VT : A.A. Balkema, ISBN 9054107634.

34. **Grigoryan, A. A. (2005).** " On certain characteristic design features of pile foundations in soils classed as type II in terms of proneness to slump-type settlement," Osn., Fundam. Mekh. Gruntov, No. 1, pp. 21-25.

35. **Hanna, A.M., and Sharif A. (2006).** "Drag force on a single pile in clay subjected to surcharge loading". International Journal of Geo-mechanics, ASCE, 6 (2), pp. 89-96.

36. **Houston, L. S., Houston, W. N., and Spandola, D. J. (1988).** "Prediction of Collapse of Soils due to Wetting," Journal of Geotechnical Engineering, 114(1).

37. **Houston, S.L. and Houston, W.N. (1997).** "Collapsible Soil Engineering". Unsaturated Soil Engineering Practice, Geotechnical Special Publication No. 68, ASCE, (edited by Houston and Fredlund).

38. **Jennings, J. E., and Knight, K. (1975).** "A guide to construction on or with material exhibiting additional settlement due to collapse of grain structure." Proc., 6t^{h} Regional Conf. of Africa on SMFE, 99–105.

39. **Johannessen, I.J., and Bjerrum, L. (1965).** "Measurement of the compression of a steel pile to rock due to settlement of the surrounding clay". In Proceedings of the 6th International Conference on Soil Mechanics and Foundation Engineering, Montréal, Que., 8–15 September 1965. Pergamon Press, Oxford, UK. pp. 261–264.

40. **Kalashnikova, O. P. (1976).** "Investigation of the behavior of piles in a collapsible soil stabilized through a leading hole." Soil Mechanics and Foundation Engineering journal, Vol. 13, No. 1, pp. 16-19.

41. **Keenan, G.H., and Bozozuk, M., (1985),** "Downdrag on three-pile group of pipe piles". In: (2nd edn. ed.), Proc. 11th Int. Conf. Mech. & Found. Engng. Vol. 3 pp. 1407–1412.

42. **Knight, K. (1963).** "The origin and occurrence of collapsing soils." Proc., 3rd Regional Conf. of Africa on SMFE, pp. 127–130.

43. **Krutov, V. I. (2003).** "Consideration of additional loading on piles due to forces of loading friction in soils prone to slump-type settlement,". Osn., Fundam. Mekh. Gruntov, No. 6, pp. 23-27.

44. **Lee, C. Y., (1993).** ''Pile groups under negative skin friction.'' J. Geotech. Eng., 119(10), pp. 1587–1600.

45. **Lee, C.J., Bolton, M.D., and Al-Tabaa, A. (2001).** "Recent findings on negative skin friction in piles and pile groups in consolidating ground" 5th Internation Conference on Deep Foundation Practice, Singapore, April, pp. 273-280.

46. **Lee, C.J., Bolton, M.D., and Al-Tabbaa, A., (2002).** "Numerical modelling of group effects on the distribution of dragloads in pile foundations". Geotechnique 52 5, pp. 325–335.

47. **Leung, C.F., Radhakrishnan, R., and Tan, S.A., (1991).** "Performance of precast driven piles in marine clay". ASCE Journal of Geotechnical Engineering, Vol. 117, No. 4, pp. 637 – 657.

48. **Little, J. A. & Ibrahim, K. I. (1993).** "Predictions associated with the pile downdrag study at the SERC soft clay site at Bothkennar, Scotland". In Predictive Soil Mechanics (Wroth Memorial Symposium), pp. 796–818.

49. **Mansur, C. I. , and Focht, J. A. ,(1953)** "Pile-Loading Tests, Morganza Floodway. Control Structure", Proceedings, ASCE, Vol. 79, paper No.324, pp. 324-1-31.

50. **McCammon, N.R., and Golder, H.Q. (1970).** "Some loading tests on long pipe piles". Géotechnique, 20, pp. 171–184.

51. **McClelland B., (1974).** "Design of deep penetration piles for ocean structures". J Geotech Eng Divis ASCE 100(GT7), pp. 709–747

52. **Meyerhof, G.G. (1976).** "Bearing Capacity and settlement of pile foundations". The Eleventh Terzaghi Lecture (1975) November 5, Journal of the Geotechnical Engineering Division, ASCE, 102 (GT3), pp. 195-228.

53. **Peck, R.B., (1958).** "A study of the comparative behaviour of friction piles". Special Report 36, Highway Research Board, Washington, D.C., pp. 1-72.

54. **Pengelly, A., Boehm, D., Rector, E. and Welsh, J. (1997).** "Engineering Experience with in Situ Modifcation of Collapsible and Expansive Soils." Unsaturated Soil Engineering, ASCE, Special Geotechnical Publication.

55. **Poulos, H.G. (1997).** "Piles subjected to negative friction: A procedure for design". Geotechnical Engineering (Southeast Asian Geotechnical Society), 28(1), pp. 23–44.

56. **Poulos, H. G., and Davis, E. H. (1980).** "Pile foundation analysis and design". Wiley, New York.

57. **Rollins, K. and Rogers, G.W. (1994).** "MitigationMeasures for Small Structures on Collapsible Alluvial Soils", J. Geot. Engr., ASCE, 120(9).

58. **Teh, C. I., and Wong, K. S. (1995).** "Analysis of downdrag on pile groups." Geotechnique, 45(2), pp. 191–207.

59. **Terzaghi, K., and Ralph B. Peck, (1948).** "Soil Mechanics in Engineering Practice", 1st Edition, John Wiley and Sons, New York, pp.456-483.

60. **Tomlinson, M.J., (1957).** "The adhesion of piles driven in clay soils". Proceedings, 4th International Conference on SoilMechanics and Foundation Engineering, London, Vol. 2, pp. 66–71.

61. **Turnbull, W. (1968).** "Construction Problem Experiences with Loess Soils." Hwy. Research Record, No. 212.

62. **Walker, L. K. and Darwall, P, (1973).** "Drag-Down on coated and uncoated piles". Proceedings of the 8th International Conference on Soil Mechanics and Foundation Engineering, Moscow, Vol. 2.2, pp. 257 - 262.

63. **White, J.L., (2006).** "Characteristics and Susceptibility of Collapsible Soils in Colorado: Results of a Statewide Study". GEO-Volution: The Evolution of Colorado's Geological and Geotechnical Engineering Practice (GSP 4), pp. 86-98.

64. **York, D. L., Miller, V. G., and Ismael, N. F., (1975)** "Long-Term Load Transfer in End Bearing Pipe Piles," Canadian Geotechnical Journal, Vol. 12.